Assessing trade-offs among electrification and grid decarbonization in a clean energy transition: Application to New York State

Terence Conlon[a†*], Michael Waite[a†**], Yuezi Wu[a***], and Vijay Modi[a****]

[a]Department of Mechanical Engineering, Columbia University
220 S.W. Mudd Building, 500 West 120th Street, New York, NY 10027, USA

[†] Corresponding author
* tmc2180@columbia.edu
** mbw2113@columbia.edu
*** yw3054@columbia.edu
**** modi@columbia.edu

Abstract

A modeling framework is presented to investigate trade-offs among decarbonization from increased low-carbon electricity generation and electrification of heating and vehicles. The model is broadly applicable but relies on high-fidelity parameterization of existing infrastructure and anticipated electrified loads; this study applies it to New York State where detailed data is available. Trade-offs are investigated between end use electrification and renewable energy deployment in terms of supply costs, generation and storage capacities, renewable resource mix, and system operation. Results indicate that equivalent emissions reductions can be achieved at lower costs to the grid by prioritizing electrification with 40-70% low-carbon electricity supply instead of aiming for complete grid decarbonization. With 60% electrification and 50% low-carbon electricity, approximately 1/3 emissions reductions can be achieved at current supply costs; with only 20% electrification, 90% low-carbon electricity is required to achieve the same emissions reductions, resulting in 43% higher grid costs. In addition, three primary cost drivers are identified for a system undergoing decarbonization: (1) decreasing per-unit costs of existing infrastructure with increasing electrified demand, (2) higher in-state generation costs from low-carbon sources relative to gas-based and hydropower generation, and (3) increasing integration costs at high percentages of low-carbon electricity.

Keywords

Decarbonization; Heating and vehicle electrification; Low-carbon electricity; Energy system modeling; New York State.

Nomenclature

Fixed variables and parameters

$A_{P_x,j}$	capital annualization rate for annualization period *P*, technology *x*, and interest rate *j* [years^{-1}]
$C_{existing-cap}$	total cost of existing transmission and generation capacity over entire analysis period [$]
$C_{generation}$	total generation cost over entire analysis period [$]
$C_{new-cap}$	total new capacity cost over entire analysis period [$]
$c_{bio,i}$	biofuel generated electricity price at node *i* [$/MWh]
$c_{existing-ramp}$	existing fossil fuel-based generation ramping cost [$/MW-h]
$c_{ff,i}$	fossil fuel price at node *i* [$/MMBTU]
$c_{hydro,i}$	hydropower generated electricity price at node *i* [$/MWh]
$c_{imp,i}$	imported electricity price at node *i* [$/MWh]
$c_{new-ramp}$	new fossil fuel-based generation ramping cost [$/MW-h]
$c_{nuc,i}$	nuclear generated electricity price at node *i* [$/MWh]
$CAP_{batt-e,i}$	battery storage energy capital cost at node *i* [$/MWh]
$CAP_{batt-p,i}$	battery storage power capital cost at node *i* [$/MW]
$CAP_{ff,i}$	new fossil fuel-based generation capital cost at node *i* [$/MW]
$CAP_{on,i}$	onshore wind power capital cost at node *i* [$/MW]
$CAP_{off,i}$	offshore wind power capital cost at node *i* [$/MW]
$CAP_{us-solar,i}$	utility-scale solar generation capital cost at node *i* [$/MW]
$CAP_{tx,ii'}$	capital cost of upgraded transmission from node *i* to adjacent node *i'* [$/MW-mi]
$D^t_{elec,i}$	existing electricity demand at node *i* and timestep *t* [MWh]
$D^t_{heat,i}$	electrified heating demand at node *i* and timestep *t* [MWh]
$D^{t,full}_{heat,i}$	full electrified heating demand at node *i* and timestep *t* [MWh]
$D^{t,full}_{veh,i}$	full electric vehicle charging demand at node *i* and timestep *t* [MWh]
$d_{ii'}$	distance between node *i* and adjacent node *i'* [mi]
$EX_{cap,i}$	annual cost of maintaining existing generation capacity at node *i* [$/MW-yr]
$EX_{tx,i}$	annual cost of existing transmission at node *i* [$/MWh-yr]
F	quantity of fuel consumed [MJ]
$H^t_{fix,i}$	fixed hydropower electricity generation at node *i* and timestep *t* [MWh]
$H^{max}_{flex,i}$	flexible hydropower maximum electricity generation at node *i* [MWh]
I	set of all nodes in study region
i	single node in the study region
i'	node adjacent to *i*
j	interest rate
l	transmission loss rate
N^t_i	nuclear-generated electricity at node *i* [MWh]
n_{years}	number of years in the analysis [years]

omf_{ff}	new fossil fuel-based generation fixed operations and management cost [$/MW-yr]
omf_{on}	onshore wind power fixed operations and management cost [$/MW-yr]
omf_{off}	offshore wind power fixed operations and management cost [$/MW-yr]
$omf_{us-solar}$	utility-scale solar power fixed operations and management cost [$/MW-yr]
$omf_{tx,ii'}$	fixed operations and management cost of upgraded transmission from node *i* to adjacent node *i'* [$/MW-yr]
omv_{ff}	new fossil fuel-based generation variable operations and management cost [$/MWh]
P	annualization period [years]
t	hourly time step
T	total number of hourly time steps in analysis
$U_{tx-flow,i}^{existing}$	annual existing intranodal transmission flow at node *i* [MWh]
$W_{off,i}^{t}$	potential offshore wind-generated electricity at node *i* and timestep *t* [$MWh_{generation}/MW_{installed}$]
$W_{on,i}^{t}$	potential onshore wind-generated electricity at node *i* and timestep *t* [$MWh_{generation}/MW_{installed}$]
$W_{btm-solar,i}^{t}$	potential behind-the-meter solar-generated electricity at node *i* and timestep *t* [$MWh_{generation}/MW_{installed}$]
$W_{us-solar,i}^{t}$	potential utility-scale solar-generated electricity at node *i* and timestep *t* [$MWh_{generation}/MW_{installed}$]
$X_{btm-solar,i}$	capacity of behind-the-meter solar generation (existing and newly simulated) at node *i* [MW]
$X_{cap,i}^{existing}$	capacity of existing generation with associated maintenance costs at node *i* [MW]
$X_{off,i}^{existing}$	capacity of existing offshore wind generation at node *i* [MW]
$X_{on,i}^{existing}$	capacity of existing onshore wind generation at node *i* [MW]
$X_{us-solar,i}^{existing}$	capacity of existing utility-scale solar generation at node *i* [MW]
$\eta_{ff-existing}$	fossil fuel-based generation efficiency of existing capacity
η_{ff-new}	fossil fuel-based generation efficiency of new capacity
ε	emissions [CO_2e]
θ	emissions rate [CO_2e/unit energy]

Decision variables
All variables are constrained to be greater than or equal to 0.

$D_{veh,i}^{t}$	vehicle charging demand at node *i* and timestep *t* [MWh]
$H_{flex,i}^{t}$	flexible hydropower electricity generation at node *i* and timestep *t* [MWh]
$G_{existing,i}^{t}$	fossil fuel-based generation from existing capacity at node *i* and timestep *t* [MWh]

$G^t_{existing-diff,i}$	absolute value of the difference in fossil fuel-based generation from existing capacity at node *i* between time steps *t* and *t-1* [MWh]
$G^t_{new,i}$	fossil fuel-based generation from new capacity at node *i* and timestep *t* [MWh]
$G^t_{new-diff,i}$	absolute value of the difference in fossil fuel-based generation from new capacity at node *i* between time steps *t* and *t-1* [MWh]
L^t_i	biofuel generation at node *i* and timestep *t* [MWh]
V^t_i	imported electricity at node *i* and timestep *t* [MWh]
$X_{batt-e,i}$	battery storage energy capacity installed at node *i* [MWh]
$X_{batt-p,i}$	battery storage power capacity installed at node *i* [MW]
$X_{ff,i}$	capacity of fossil fuel-based generation installed at node *i* [MW]
$X_{off,i}$	capacity of offshore wind generation installed at node *i* [MW]
$X_{on,i}$	capacity of onshore wind generation installed at node *i* [MW]
$X_{us-solar,i}$	capacity of utility-scale solar generation installed at node *i* [MW]
$X_{tx,ii'}$	capacity of new transmission from node *i* to adjacent node *i'* [MW]
$Z^t_{ii'}$	electricity transmitted from node *i* to adjacent node *i'* at timestep *t* [MWh]
$\gamma^t_{batt,i}$	increase in battery storage state of charge at node *i* and timestep *t* [MWh]
$\delta^t_{batt,i}$	decrease in battery storage state of charge at node *i* and timestep *t* [MWh]

Scenario configuration parameters

LCP	low-carbon electricity generation percent: Fraction of total demand that must be met by low-carbon energy (combined nuclear, wind, water, and solar power)
$p_{heat,i}$	fraction of full heating electrification demand simulated at node *i*
$p_{veh,i}$	fraction of full vehicle electrification demand simulated at node *i*
ω	percent reduction in total greenhouse gas emissions

Subscripts and superscripts

(Note: Some fixed variables and parameters defined above are used in subscripts and superscripts. These terms are not redefined here.)

batt	battery storage
bio	biofuel
btm	behind-the-meter
diff	difference
elec	electricity
fix	fixed
ff	fossil-fuel
flex	flexible
heat	heating
imp	imports
ind	industrial sector
off	offshore wind
on	onshore wind

other	out-of-scope
p2e	power-to-energy
tot	total
transp	transportation sector
tx	transmission
us	utility scale
veh	vehicle

Acronyms

SECTR	System Electrification and Capacity TRansition
SECTR-NY	System Electrification and Capacity TRansition – applied to New York State
HVE	heating and vehicle electrification
GHG	greenhouse gas
LCOE	levelized cost of electricity
CEM	capacity expansion model
RTO	regional transmission organization
ISO	independent system operator
NYS	New York State
NREL	National Renewable Energy Laboratory
VRE	variable renewable energy

1. Introduction

The United States is at a clean energy crossroads. Economically, per-unit costs of new solar and wind generation have become lower than coal and gas generation in parts of the country [1]. Policy-wise, several states have recently passed major climate legislation [2]. Public opinion mirrors these changes: A growing consensus acknowledges that a clean energy transition would have numerous social [3] and economic benefits [4]. As a result, support for sweeping federal action has reached new heights [5]. Even so, the cost-effectiveness of this transition will be influenced by region-specific nuances of legacy infrastructure, energy sources, and constraints [6]. This paper proposes an open-source framework that offers a means to evaluate decarbonizing the electricity grid while considering electrification of heating and vehicles. The framework is then to New York State (NYS) to highlight trade-offs among dominant decarbonization options emblematic of a region with a well-defined electricity system and a variety of climates, renewable energy resources, and existing fossil fuel end use needs.

There is widespread consensus that coupling electrification of heating and vehicles with renewable energy expansion is the best approach to reducing energy-related greenhouse gas (GHG) emissions [7]. In fact, it is infeasible to meet deep decarbonization targets without both cleaning the grid and replacing current fossil fuel transportation and heating technologies with low-carbon alternatives [8]. However, less well understood are how prioritizing fossil fuel end use electrification or the percentage of electricity from low-carbon sources influences the cost-effectiveness of emissions reductions, electrification's potential benefits to the electricity system, and how transitioning existing heating and transportation infrastructure impacts hourly energy system operation.

Many energy system models seek to determine economically optimal technology mixes for future electricity scenarios, including those set in NYS [9]. Modeling unit commitment and dispatch [10] at the scale of individual generators [11] under varying degrees of foresight [12] can provide detailed operational understanding for a fully defined system. Capacity expansion models (CEMs) generally aggregate generators with similar characteristics in order to avoid the significant computational requirements of high spatial and temporal resolution models with capacities as decision variables [13]. The improved tractability of CEMs (often called "macro-energy system models"[14] when applied to regional systems) allows them to incorporate a larger number of system characteristics [15]. CEMs have expanded to include additional technological options, demonstrating that higher fidelity to existing systems results in more accurate capacity expansion scenarios [16]. By modeling resource stochasticity, other CEMs find that optimal system design changes under uncertainty [17]. Moreover, the inclusion of environmental considerations shifts the deployment of renewable generation capacity compared to CEMs that do not account for land-use limitations [18]. CEMs that simulate interconnected energy systems such as transportation [19] and heating [20] have modeled sector-wide clean energy transitions, showing that the interplay of different energy demands is critical in understanding decarbonization pathways. Nevertheless, because characterizing actual systems can be time-consuming (if sufficient information and data is even available), CEMs often do not contain high-fidelity

parameterizations of all existing system conditions [20]. These shortcomings are particularly problematic for regional energy systems (e.g. at the Regional Transmission Organization (RTO) or Independent System Operator (ISO) scale) with unique existing infrastructure and resource mixes that are likely to affect deep decarbonization efforts, as well as intra-regional heterogeneity that may not be captured in larger-scale models [21].

While CEMs have previously been used to investigate the impact of electrified loads on least-cost model decisions, there remain opportunities for improvements in methods and applications. A group of CEM-based studies by the U.S. National Renewable Energy Laboratory (NREL) explores the effects of electrification and decarbonization on model-selected energy infrastructure capacities [22], electricity cost [23], emissions [24], variable renewable electricity (VRE) integration [25], and electricity demand curves [26] in the continental US. These NREL studies use representative time slices in place of continuous time series to solve models with high spatial resolution, but this approach precludes thorough investigation of system operation. Similarly, a recent study on achieving net-zero emissions in the continental U.S. through expanded low-carbon electricity and end use electrification simulates power sector operations at an hourly resolution for 41 representative days [21]; as with the NREL studies, representative time slices prevent a full accounting for system operation over a continuous time period. Other studies include continuous supply and demand time series to evaluate power flow for discrete scenarios (i.e. with fixed infrastructure capacities rather than optimal capacity expansion decision-making) to evaluate the effects of electrification on VRE integration [27]. Another study of this type applies a grid model introduced in [28] to evaluate the effects of electrified heating demand in California on both GHG emissions and grid resource capacity needs. Here, resource mixes are exogenously defined, and electricity costs in future electrification scenarios are not presented [29].

Recent studies of NYS have found that deep decarbonization is feasible using existing technologies, and that different pathways exist to a carbon neutral future [30]. One such report issued by New York's Climate Action Council concludes that substantial progress on heating and vehicle electrification is required by 2030, and that nearly 100 GW of renewable generation capacity is required for full energy sector decarbonization by 2050 [31]. Related work uses a capacity expansion model and representative timeseries to show that battery storage will be required to ensure electricity reliability during a low-carbon transition [32]. However, these studies also list areas for future research, including incorporation of an updated GHG emissions assumptions accounting [30].

A gap in the literature thus remains: An evaluation of both cost-optimal capacity expansion and system operation for a well-characterized existing regional energy system, under various combinations of electrification and low-carbon electricity adoption rates, using multiple years of real data, with improved emissions assumptions. This paper addresses this gap by introducing an open-source System Electrification and Capacity TRansition (SECTR) modeling framework. To determine optimal system characteristics, SECTR computes the lowest total cost of electricity generation, transmission, and storage resource mix for specified combinations of: (a) low-carbon electricity supply percentage, (b) building end use and vehicle electrification, and (c) percent GHG

emissions reduction. SECTR is designed to replicate existing system characteristics: spatially heterogeneous hourly electricity demands, generation technologies, and capital and operating costs; inter-nodal transmission limits; energy storage; temperature-dependent electric vehicle charging demands; and electrified heating demand time series [33]. Agriculture and industrial emissions are included in GHG computations, but SECTR does not endogenously model changes in those sectors. In this paper, the SECTR framework is applied to New York State's energy system (SECTR-NY). Lastly, for the SECTR-NY application, this paper includes an emissions accounting that improves upon the accounting contained in current NYS reports, as it incorporates methane leakage and adopts the longer duration GHG warming potentials specified by a recent state climate law.

2. Methodology

Section 2 contains a description of the SECTR model general formulation, and the motivation for its application to New York State. All modeling information not specified in Section 2 is contained in Section S2 of the Supplementary Materials.

2.1 System Electrification and Capacity Transition model general formulation

A SECTR model study region is defined by individual nodes, *i,* representing geographical sub-areas within the larger region of interest. Along with existing electricity demand, each node contains electrified heating[i] and vehicle charging loads at each timestep, *t*, within the overall time period simulated, *T.* To determine the least-cost infrastructure mix in future model scenarios, decision variables are assigned node-specific costs. SECTR uses a characterization of the region's energy-related GHG emissions as both a reference quantity for GHG emissions reduction computations and to compute the emissions impact of reduced fossil fuel usage associated with heating and vehicle electrification; the model does not consider improved efficiency or growth of fossil fuel end uses.

SECTR evaluates different low-carbon electricity supply and end use electrification scenarios by computing the total cost of new and existing infrastructure capacity and maintenance, fuels, and resource operation to estimate the total annual cost of electricity generation and transmission; these returned costs do not include delivery expenses (primarily distribution system costs). The modeling framework does not include the cost of replacing current fossil fuel-based building systems and vehicles or electricity distribution system costs; as such, SECTR cost computations can be considered those that typically constitute the "supply" portion of a utility customer's bill.

The remainder of Section 2.1 contains a subset of the SECTR governing equations that establish the model configuration, along with additional equations that define how costs and emissions are calculated. Due to space constraints, Section S2 of the Supplementary Materials presents the remainder of the SECTR governing equations, including those constraining fossil fuel generation, wind capacity, solar capacity, internodal transmission, battery storage, nuclear generation, hydropower generation, biofuel generation, interregional exports, and additional generation capacity costs.

Objective function

SECTR's objective function minimizes the total annual electricity system supply cost based on specification of two of the following three configuration parameters: (1) minimum percent of in-state electricity generated from low-carbon resources, LCP; 2) minimum percent electrification

[i] Note that SECTR incorporates the ability to model shifts of any fossil fuel-based building end use, which generally depend on heat in some form: In US residences, 93% of natural gas, 86% of propane, and 98% of fuel oil consumption is used for either space or water heating [44]; in commercial buildings, 78% of natural gas and 70% of fuel oil consumption is used for space or water heating [45]. As such, "heating" is used for short.

of current fossil fuel-based heating, p_{heat}, and vehicle electrification, p_{veh}; and (3) minimum GHG emissions reduction requirement, ω. Eqs. (1-4) describe the objective function, where $C_{new-cap}$ is the total cost of new capacity, $C_{generation}$ is the total cost of generation, and $C_{existing-cap}$ is the total cost of maintaining existing capacity:

$$obj = \ minimize\left(C_{new-cap} + \ C_{generation} + \ C_{existing-cap}\right) \tag{1}$$

$$\begin{aligned} C_{new-cap} = n_{years} & \\ & * \sum_{i \in I} \Big[(A_{P_{on},j} * CAP_{on,i} + \ omf_{on}) * X_{on,i} \ + \ (A_{P_{off},j} * CAP_{off,i} + \ omf_{off}) \\ & * X_{off,i} \ + \ (A_{P_{us-solar},j} * CAP_{us-solar,i} + \ omf_{us-solar}) * X_{us-solar,i} \\ & + \ (A_{P_{batt},j} * CAP_{batt-e,i}) * X_{batt-e,i} \ + \ \ (A_{P_{batt},j} * CAP_{batt-p,i}) * X_{batt-p,i} \\ & + \ (A_{P_{ff},j} * CAP_{ff,i} \ + omf_{ff}) * X_{ff,i} \\ & + \ \sum_{i'} (A_{P_{tx},j} * CAP_{tx,ii'} * d_{ii'} + omf_{tx,ii'}) * X_{tx,ii'} \Big] \end{aligned} \tag{2}$$

$$\begin{aligned} C_{generation} = \sum_{i \in I} \sum_{t \in T} \Big[& c_{hydro,i} * \left(H^t_{fixed,i} + \ H^t_{flex,i}\right) + \ c_{nuc,i} * N^t_i \ + \ c_{bio,i} * L^t_i \ + \ c_{imp,i} * V^t_i \\ & + \ 3.412 * c_{ff,i} * \left(\frac{G^t_{existing,i}}{\eta_{ff-existing}} + \frac{G^t_{new,i}}{\eta_{ff-new}} \right) + \ omv_{ff} * G^t_{new,i} + \ c_{existing-ramp} \\ & * G^t_{existing-diff,i} + \ c_{new-ramp} * G^t_{new-diff,i} \Big] \end{aligned} \tag{3}$$

$$C_{existing-cap} = \ n_{years} * \sum_{i \in I} \left[EX_{cap,i} * X^{existing}_{cap,i} \ + \ EX_{tx,i} * \ U^{existing}_{tx-flow,i} \ \right] \tag{4}$$

Levelized cost of electricity calculations

The levelized cost of electricity (LCOE) is calculated per Eq. (5):

$$LCOE = \frac{C_{new-cap} + \ C_{generation} + \ C_{existing-cap}}{\sum_{t \in T} \sum_{i \in I} \left[\mathrm{D}^t_{elec,i} + \ \mathrm{D}^t_{heat,i} + \ \mathrm{D}^t_{veh,i} - \ X_{btm-solar,i} \ * \ W^t_{btm-solar,i} \right]} \tag{5}$$

Note that the LCOE is simply the total electricity supply cost divided by the total electricity demand, after subtracting contributions from behind-the-meter (BTM) solar generation. LCOE is used as a general comparative metric between scenarios.

Capital cost annualization

For a given technology, *x*, the annualization rate ($A_{P_x,j}$) associated with the capacity cost, CAP_x, is computed from a technology-specific annualization period (P_x) and a 5% interest rate (j), per Eq. (6).

$$A_{P_x,j} = \frac{j * (1+j)^{P_x}}{((1+j)^{P_x} - 1)} \tag{6}$$

Heating and vehicle electrification

Hourly demands for electrified heating, $D^t_{heat,i}$, are based on the nodal percentage of heating electrification, $p_{heat,i}$, and user-provided nodal electricity demands for full heating electrification, $D^{t,full}_{heat,i}$, per Eq. (7).

$$D^t_{heat,i} = p_{heat,i} * D^{t,full}_{heat,i} \tag{7}$$

Electric vehicle demand at each time step, $D^t_{veh,i}$, is based on the nodal percentage of vehicle electrification, $p_{veh,i}$, and user-provided nodal electricity demands for full vehicle electrification, $D^{t,full}_{veh,i}$, per Eq. (8).

$$D^t_{veh,i} = p_{veh,i} * D^{t,full}_{veh,i} \tag{8}$$

Energy balance constraint

The nodal energy balance is constrained by the following inequality, with all variables defined in the Nomenclature:

$$\begin{aligned}(X_{on,i} + X^{existing}_{on,i}) * W^t_{on,i} + (X_{off,i} + X^{existing}_{off,i}) * W^t_{off,i} + (X_{us-solar,i} + X^{existing}_{us-solar,i}) \\ * W^t_{us-solar,i} + X_{btm-solar,i} * W^t_{btm-solar,i} + H^t_{flex,i} + H^t_{fixed,i} + N^t_i \\ + G^t_{existing,i} + G^t_{new,i} + L^t_i + V^t_i - \gamma^t_{batt,i} + \delta^t_{batt,i} \\ + \sum_{i'} [(1-l) * Z^t_{i'i} - Z^t_{ii'}] \geq \mathrm{D}^t_{elec,i} + \mathrm{D}^t_{heat,i} + D^t_{veh,i}\end{aligned} \tag{9}$$

The low-carbon electricity generation curtailment is computed from the slack in this constraint at each node.

Low-carbon electricity generation targets

For certain SECTR configurations, the user selects a low-carbon percent (LCP) – a minimum percentage of in-state electricity supply from onshore and offshore wind, hydropower, solar, and nuclear power after subtracting out contributions from BTM generation; the electricity generated from fossil fuels and biofuels over the full simulation period is thus constrained per Eq. (10).

$$\sum_{t\in T}\sum_{i\in I}\left(G^t_{existing,i} + G^t_{new,i} + L^t_i\right) \leq (1 - LCP) * \sum_{t\in T}\sum_{i\in I}\left[\mathrm{D}^t_{elec,i} + \mathrm{D}^t_{heat,i} + \mathrm{D}^t_{veh,i} - V^t_i - X_{btm-solar,i} * W^t_{btm-solar,i}\right] \quad (10)$$

Emission reduction calculations and assumptions

In-region electricity generation emissions are calculated with emissions rate of fossil fuel-based generation, θ_{ff}, and generation from existing, $G^t_{existing,i}$, and new, $G^t_{new,i}$, fossil fuel plants, after accounting for their respective efficiencies, $\eta_{ff-existing}$ and η_{ff-new}. Emissions from imported electricity are determined by the product of the emissions rate of imports, $\theta_{imp,i}$, and the quantity of imports, V^t_i. Together, emissions from in-region generated electricity and imports are summed over all nodes *i* and timesteps *t* to compute total electricity related GHG emissions, ε_{elec}, for each scenario, per Eq. (11).

$$\varepsilon_{elec} = \sum_{t\in I}\sum_{i\in I}\left[\theta_{ff} * \left(\frac{G^t_{existing,i}}{\eta_{ff-existing}} + \frac{G^t_{new,i}}{\eta_{ff-new}}\right) + \theta_{imp,i} * V^t_i\right] \quad (11)$$

GHG emissions of remaining fossil fuel heating, ε_{heat}, are equal to product of the complement of the heating electrification fraction simulated, $p_{heat,i}$; the blended emissions rate for heating, θ_{heat}; and the total quantity of heating fuel consumed $F_{heat,tot,i}$. This quantity is summed over all nodes *i* and is computed per Eq. (12):

$$\varepsilon_{heat} = \sum_{i\in I}\left(1 - p_{heat,i}\right) * \theta_{heat} * F_{heat,tot,i} \quad (12)$$

GHG emissions of non-electrified vehicles, ε_{veh}, are calculated per Eq. (13). This accounting is analogous to that for heating emissions, using the fraction of vehicle electrification simulated, $p_{veh,i}$; the blended emissions rate for vehicles, θ_{veh}; and the total quantity of vehicle fuel consumed, $F_{veh,tot,i}$. Total transportation sector emissions also include existing transportation emissions outside the scope of the current analysis, $\varepsilon_{transp,other}$, per Eq. (14):

$$\varepsilon_{veh} = \sum_{i \in I} \left(1 - p_{veh,i}\right) * \theta_{veh} * F_{veh,tot,i} \tag{13}$$

$$\varepsilon_{transp} = \varepsilon_{veh} + \varepsilon_{transp,other} \tag{14}$$

Industrial sector emissions from energy consumption, ε_{ind}, are added to compute total GHG emissions. Emissions from the incineration of waste are excluded from the specific formulations of future energy scenarios. To compute the overall percent reduction in GHG emissions, ω, SECTR compares total computed emissions to the user-provided reference quantity, $\varepsilon_{reference}$ per Eq. (15).

$$\omega = \frac{\varepsilon_{reference} - (\varepsilon_{elec} + \varepsilon_{heat} + \varepsilon_{transp} + \varepsilon_{ind})}{\varepsilon_{reference}} \tag{15}$$

Fig. 1 presents a flowchart that summarizes the main steps for a user – broadly defined as anyone defining or executing a SECTR configuration – to instantiate and solve SECTR model scenarios. In short, after defining the fixed variables and parameters (see *Nomenclature*), specifying two of the three scenario configuration parameters – low-carbon electricity percent, LCP; heating and vehicle electrification (HVE) rates p_{heat} and p_{veh}; and GHG reduction, ω – allows SECTR to determine the cost-optimal energy system design for a future decarbonization scenario.

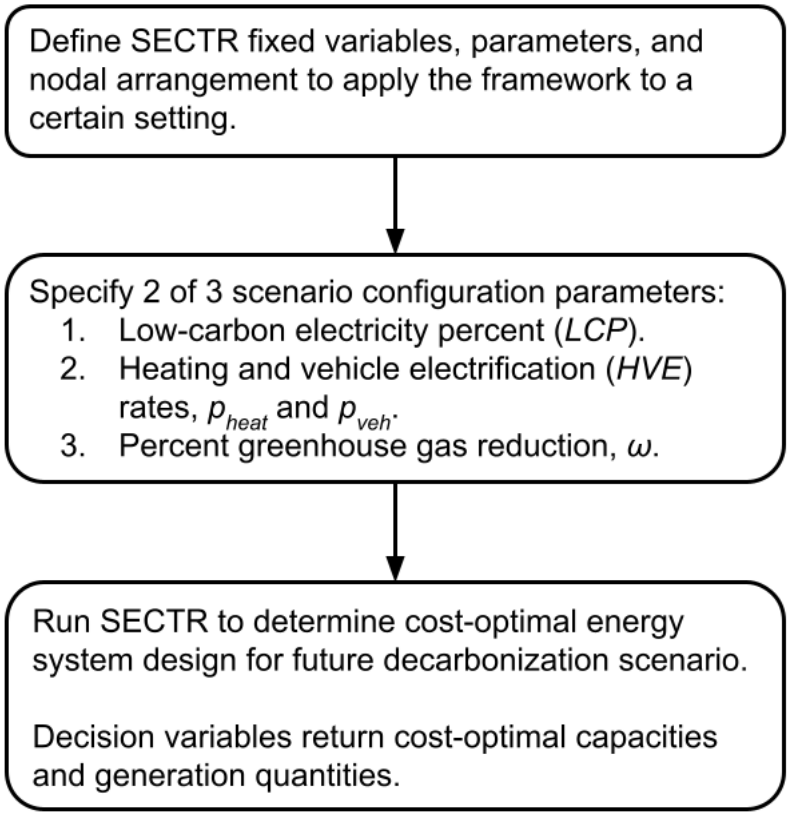

Fig 1: Flowchart for instantiating and solving SECTR general formulation model scenarios.

2.2 Application to New York State

This paper applies the SECTR framework to New York State (SECTR-NY), which provides a useful study area for several reasons, including:

- A 2019 law [34] mandating significant, quantifiable decarbonization targets in the years 2030, 2040, and 2050.
- A single electricity supply system operator and market administrator – the New York Independent System Operator (NYISO) – covering the extent of New York State.
- Well-defined transmission interfaces, both internal (between NYISO zones) and external (imports/exports between NYISO and other load areas).
- Diverse and geographically heterogeneous loads and potential renewable resources.
- Definable effects of population and built environment density on current system costs and documented costs of new infrastructure capacity.
- Extensive data availability for the current electricity system and statewide GHG emissions.

The Supplementary Materials contain a full parameterization of SECTR-NY, including descriptions of all data sources used and developed model data. Four nodes are defined for NYS by grouping NYISO zones based on the state's major transmission interfaces. The existing system is generally

defined by the most recent reference data available; however, load and weather time series data for 2007-2012 are used in the model formulation because the reference model data for hourly wind and solar resource potential are available for only those years. Monthly characteristics of electricity supply and demand time series over the six modeled years are shown in Fig. 2.

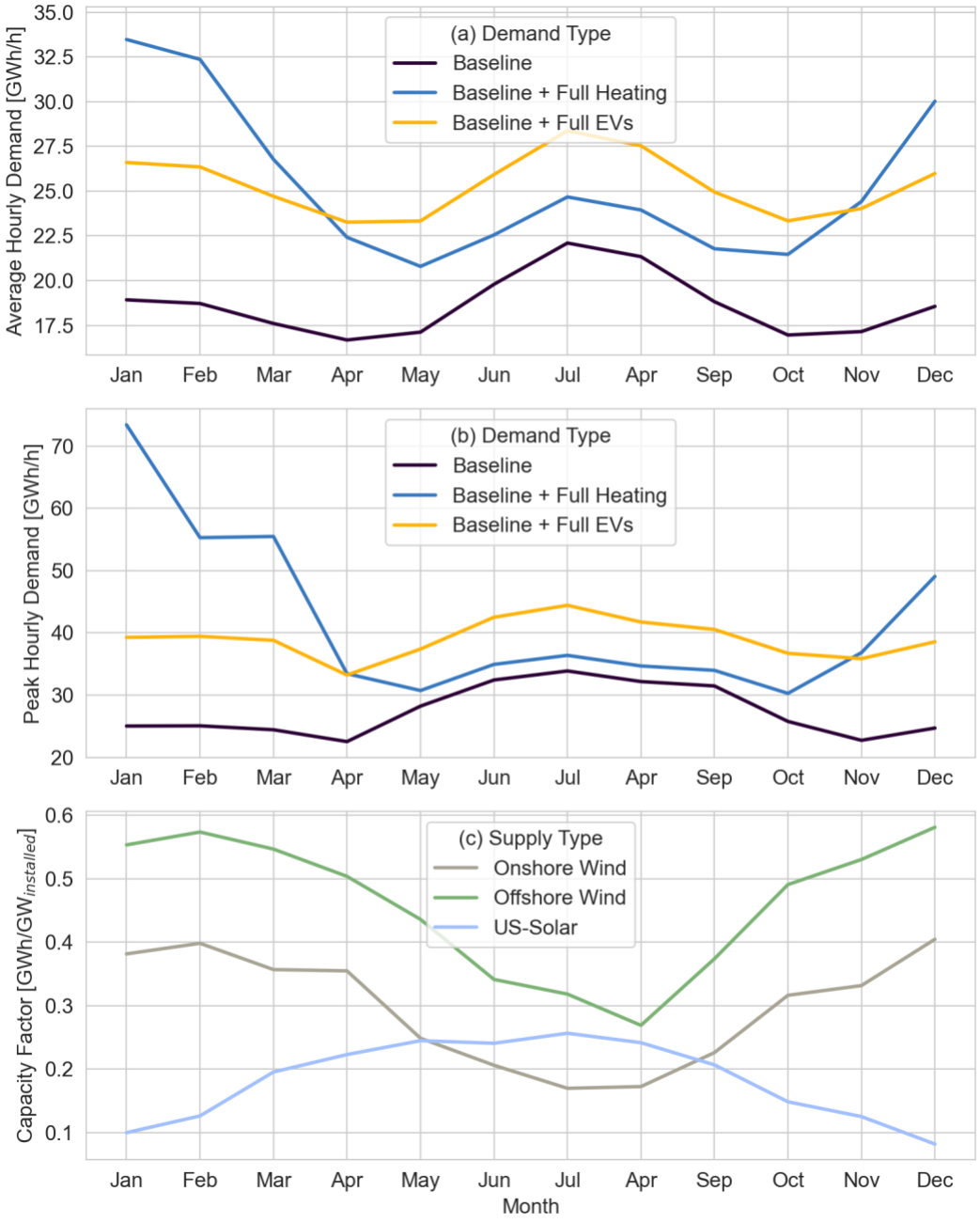

Fig. 2: (a) monthly averages of hourly electricity demand, (b) monthly peak of hourly electricity demand, and (c) monthly capacity factors for wind and solar resources in NYS.

3. Results

Section 3.1 establishes and distinguishes between a "Current" model configuration that mirrors existing NYS system characteristics, and a "Baseline" configuration for decarbonization scenario comparison. Section 3.2 presents the results of SECTR-NY Baseline configuration simulations for different combinations of in-state low-carbon electricity generation percentages (LCP) and heating and vehicle electrification rates (HVE). Section 3.3 compares SECTR-NY results to those published in recent NYS studies on decarbonization pathways. All results are presented for SECTR-NY simulations solved over the entire 6-year time period modeled; all specified generation and demand quantities are presented as hourly averages in Wh/h over the full 6-year simulation period.

3.1 Current system validation and Baseline configuration

The Baseline configuration deviates from the Current system configuration in three ways summarized in Table 1: The Baseline configuration excludes existing nuclear power at Node 1, includes an additional 5 GW of solar BTM capacity corresponding to a simulation year of 2030, and simulates an additional planned 1.25 GW of hydropower import capacity into New York City (NYC). For comparative purposes, Table 1 also includes a "Baseline with Nuclear" scenario. All Table 1 scenarios exclude any additional HVE beyond current electric heating and vehicles.

Table 1: 'Current', 'Baseline with Nuclear', and 'Baseline' system configuration comparisons.

	Configuration Parameters			Specified System Characteristics[a,b]				Model-returned System Characteristics[b]				
Configuration	% GHG[c]	% HVE[d]	% LCP[e]	Instate Hydro [GW]	Nuclear [GW]	BTM Solar [GW]	Hydro Imports [GW]	Onshore Wind [GW]	Utility-Scale Solar [GW]	Battery [GWh]	Wind and Solar LCOE [$/MWh]	Total LCOE [$/MWh]
Current	3.6	0	38.2	5.3	3.5	1.6	1.5	2.0[f]	0.1[f]	0.2[f]	69.7	65.3
Baseline w. Nuclear	-2.0	0	42.4	5.3	3.5	6.6	2.8	2.0	0.1	1.1	69.3	68.6
Baseline	-1.6	0	40	5.3	0	6.6	2.8	9.1	2.6	2.0	67.8	72.1

[a] See Supplementary Methods for existing system characteristics and the text of this section for any modifications for the specific configuration.
[b] Besides LCOE values, all system characteristics presented indicate capacities.
[c] '% GHG' refers to the percent change in greenhouse gas emissions compared to the 1990 reference quantity. A positive value indicates a computed increase in emissions, a negative value indicates a reduction.
[d] '% HVE' refers to the percent of additional heating and vehicle electrification simulated; some heating electrification (and a very small amount of vehicle electrification) currently exists in NYS.

[e] '% LCP' refers to the percent of in-state electricity supply from low-carbon sources.
[f] Indicates model capacities that are constrained to existing capacity in the 'current' configuration.

The model-computed Current configuration LCOE of $65.3/MWh compares favorably to the actual system. An actual NYS electricity supply cost of $69.1/MWh is estimated, based on 2019 NYS generation and transmission costs [35], electricity sales [35], and total zonal electricity demands; this actual cost would include ancillary service and NYISO operation costs of approximately $2/MWh [36] that are not included in SECTR-NY. Despite the difference between these two values, the close alignment in computed costs supports SECTR-NY's applicability to the NYS system and its suitability for further analyses.

The Current configuration computes an LCP of 38.2% and a 3.6% increase in GHG emissions compared to the 1990 reference quantity. Total emissions increase because CO_2 reductions from natural gas displacing coal and fuel oil combustion are offset by GHG increases from larger transportation energy demands, methane leakage associated with natural gas production and transmission, and the retirement of a large nuclear power plant; these effects are more pronounced due to the use of the 20-year GWP value for methane in place of 100-year GWP value. Moreover, the calculated LCP of 38.2% is lower than the 2019 fraction of NYS electricity demand met by low-carbon sources (62.3%) for two reasons: 1) per the language of the CLCPA, LCP only considers in-state generation, and does not account for substantial hydropower imports from Canada; and 2) SECTR-NY does not include nuclear generation from Indian Point, as this facility was fully closed on April 30, 2021[ii].

The Baseline with Nuclear configuration – adding BTM PV and NYC hydropower imports to the Current configuration – computes a 2% GHG reduction and $68.6/MWh LCOE; the $3.3/MWh higher LCOE is due to the higher cost of hydropower imported into NYC and the reduction of regional demands due to solar BTM (i.e., existing system capacity costs are distributed over less load). Removing all nuclear capacity establishes the Baseline configuration; a 40% LCP is set for round number comparison in subsequent sections that is close to the current 38.2%. Approximately 10 GW of solar and wind capacity are installed to replace the nuclear generation, resulting in a slightly lower reduction in GHG (-1.6%) and a slightly higher LCOE ($72.1/MWh). Given the reasonable deviations from the current system model, the Baseline configuration is adopted for future scenario evaluations.

3.2 Analysis of low-carbon electricity and end use electrification scenarios

For a series of SECTR-NY simulations with different combinations of LCPs and HVEs[iii], relationships among LCOE, GHG emissions, HVE, LCP, and renewable energy capacity are shown in Fig. 3. Here, computed LCOEs represent the total costs for supply (primarily generation, storage, and transmission), excluding delivery costs (primarily distribution system costs). HVE rates refer to

[ii] The "Current" and "Baseline with Nuclear" configurations do include generation from NYS nuclear plants besides Indian Point, as these plants remain operational as of this paper's publication.
[iii] In the scenarios presented, heating and vehicle electrification rates are equal.

new heating and vehicle electrification, as some heating (and a small share of vehicles) currently uses electricity. Note that the 40% LCP and 0% HVE scenario presented in Table 1 is located in the bottom-left of the figure; for comparison beyond NYS, 39.7% of US electricity generation was from low-carbon sources in 2020 [37].

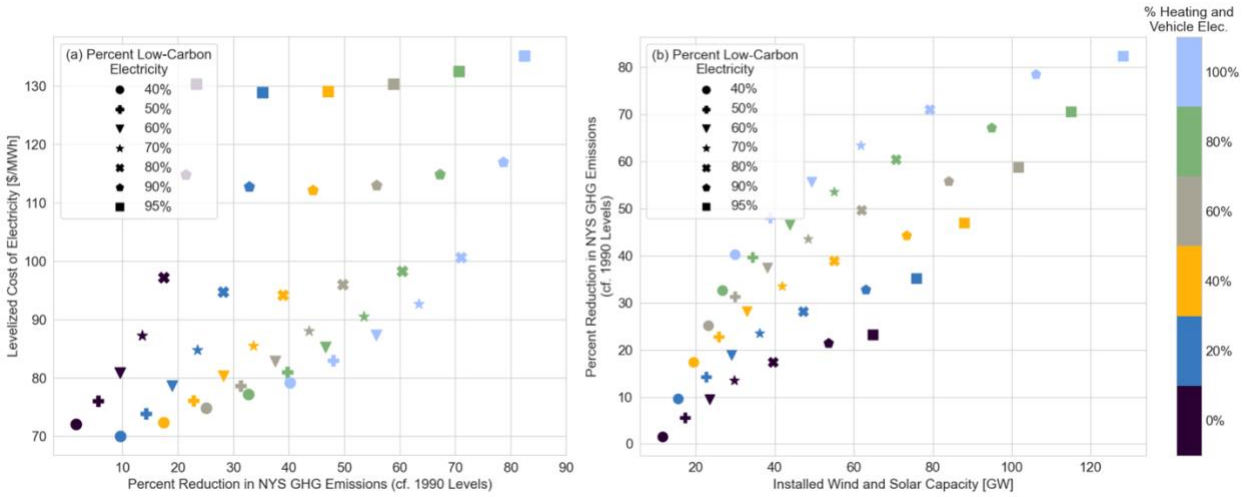

Fig. 3: (a) *LCOE vs. percent emissions reduction; (b) percent emissions reduction vs. installed wind and solar capacity. All emissions reductions are compared to 1990 levels. Marker shape indicates percent low-carbon electricity (LCP), and marker color indicates heating and vehicle electrification (HVE). All points represent independently solved SECTR-NY decarbonization scenarios with specified LCP + HVEs. For scenarios shown, all low-carbon electricity generation is from wind, solar, and hydropower.*

Fig. 3(a) shows how computed grid supply LCOE (strictly that of the electricity utilized) rises sharply with increasing LCP for a specified HVE, whereas for a specified LCP, higher HVEs cause limited growth in LCOE. Fig. 3(b) provides a partial explanation, showing that high HVE scenarios achieve the same GHG reductions with lower installed wind and solar capacities. The results suggest that emissions reductions can be achieved with a shallower initial rise in LCOE by prioritizing electrification of heating and vehicles in conjunction with deployment of solar and wind, as opposed to the latter by itself. Added loads from HVE can even slightly reduce LCOE up to a point (20-40% HVE, depending on LCP), as the additional electricity demand decreases the per-unit cost of existing infrastructure. (The same trend holds when the system includes an average of 3 GWh/h of nuclear generation in Node 1, albeit at LCOEs approximately 10% lower; see Supplementary Figure S2.)

It is worth noting the straightforward impact of HVE on GHG emissions: In NYS, a current average emissions rate for fossil fuel-based heating of 148 kgCO2e/MMBtu$_t$ (i.e. per unit heat delivered) is computed based a recent heating model [38] and GHG emissions rate assumptions described in the Supplementary Methodology; with electrified heating and 40% low-carbon electricity supply[iv] in SECTR-NY, this reduces to 44 kgCO2e/MMBtu$_t$. Similar reductions occur for vehicle electrification: A current average emissions rate for fossil fuel vehicles of 543 gCO_2e/mi (per

[iv] 40% LCP mirrors the current NYS fuel mix.

vehicle mile traveled) is computed, and 241 gCO_2e/mi for electric vehicles with 40% LCP in SECTR-NY. Therefore, even with the remaining 60% of grid power being supplied by gas-based generation, substantial reductions in overall emissions from electrification are computed.

Consider two changes in system characteristics starting at the 40% LCP and 0% HVE point of Fig. 3(a). Approximately 10% GHG emissions reductions could be achieved without additional electrification and with 60% LCP at an LCOE of $80.9/MWh; this scenario represents a 3.1 GWh/h increase in average wind and solar supply. A similar emissions reduction could be achieved with a 20% HVE and no LCP increase at a cost of $70.0/MWh; the average wind and solar supply increases by 1.1 GWh/h to maintain 40% LCP with the electrification-driven increase of 2.7 GWh/h average demand. Consider now two scenarios in Fig. 3(b) with approximately 30 GW wind and solar capacity: The scenario with 50% LCP and 60% HVE has computed GHG emissions reductions of 31%, more than double the 14% reduction in the scenario containing 70% LCP and 0% HVE. Here, the computed LCOE for the first scenario ($78.7/MWh) is nearly $10/MWh less than the second scenario ($87.2/MWh).

These various trade-offs are demonstrated with four scenarios that all contain approximately 1/3 reductions in GHG, but via different combinations of LCP and HVE. For the lowest LCP scenario shown in Table 2 (Scenario 1), GHG reductions require a high HVE that increases average load and peak load, the latter requiring larger amounts of gas turbine capacity. Comparatively, Scenario 3 contains 33 GW less gas generation capacity, accompanied by a drop in average gas generation from 15.3 GWh/h to 6.0 GWh/h. Here, higher LCP scenarios avoid increases in gas capacity and generation through additional renewable generation and battery capacity, a tradeoff that increases supply costs by $10/MWh.

Table 2: Select scenarios achieving emissions reductions of approximately 1/3 compared to the 1990 reference quantity.

Scenario	% GHG[a]	% HVE[b]	% LCP[c]	Avg. Load [GWh/h]	Wind and Solar Cap. [GW][d]	Battery Cap. [GW]	Gas Cap. [GW][e]	Avg. Gas Gen. [GWh/h][f]	LCOE [$/MWh]
1	-32.9	80	40	29.4	26.6	4.7	63.0	15.3	77.2
2	-31.3	60	50	26.7	29.8	4.2	48.9	11.4	78.7
3	-33.6	40	70	24.0	41.8	6.9	29.9	6.0	85.5
4	-32.8	20	90	21.3	63.0	15.0	27.0	1.8	112.8

[a] '% GHG' refers to the percent change in greenhouse gas emissions compared to the 1990 reference quantity. Negative values indicate reductions.

[b] '% HVE' refers to the percent of additional heating and vehicle electrification simulated; some heating electrification (and a very small amount of vehicle electrification) currently exists in NYS.

[c] '% LCP' refers to the percent of in-state electricity supply from low-carbon sources.

[d] 'Wind and Solar Cap.' refers to installed onshore wind, offshore wind, and utility-scale solar capacity.
[e] 'Gas Cap.' contains 27.0 GW existing gas-based generation capacity and model selected new gas turbines.
[f] 'Avg. Gas Gen.' refers to the average generation over the entire 6-year simulation period from existing gas-based generation and model-selected new gas turbines.

The synergy of renewable energy generation and electrification is further explained by looking at "excess low-carbon generation": Potential electricity generation from model-selected wind and solar capacities exceeding demand. Excess low-carbon generation exists as an hourly time series of either 0 MWh (when total low-carbon generation is less than the demand) or a positive value equal to the amount of low-carbon electricity generation that exceeds demand. In model simulations, excess low carbon generation must be either 1) stored for later use, or 2) curtailed. Fig. 4(a) shows that despite significant growth in renewable energy capacity with increasing HVE, excess low-carbon electricity generation remains below 6% as long as LCP does not exceed 70%; at LCP of 50% or less, excess generation is below 1%. Fig. 4(b) shows the relationship between excess low-carbon generation and LCOE for the same scenarios in Fig. 4(a).

By combining the effects discussed thus far, three primary LCOE drivers are identified: (1) decreasing per-unit costs of existing infrastructure with increasing demand from HVE, (2) higher generation costs from wind and solar power relative to existing resources, and (3) increasing integration costs when large amounts of wind and solar power produce electricity in excess of demand. Fig. 4(b) shows a general linear trend of integration costs (curtailment and battery storage) increasing LCOE at higher percents excess low-carbon generation, but also how the effects of the three cost drivers change over the entire range of LCPs and HVEs simulated. At LCPs at or below 60%, the primary cost tradeoffs discussed earlier are observed: Higher LCOEs from more wind and solar are partially mitigated by higher utilization of existing infrastructure with HVE. In the 70-80% LCP range, a transition begins in which some spread in excess low-carbon generation affects LCOE, but the first two LCOE drivers prevail. Beyond 80%, the integration cost-driven linear relationship between increasing excess low-carbon generation and computed LCOE dominate.

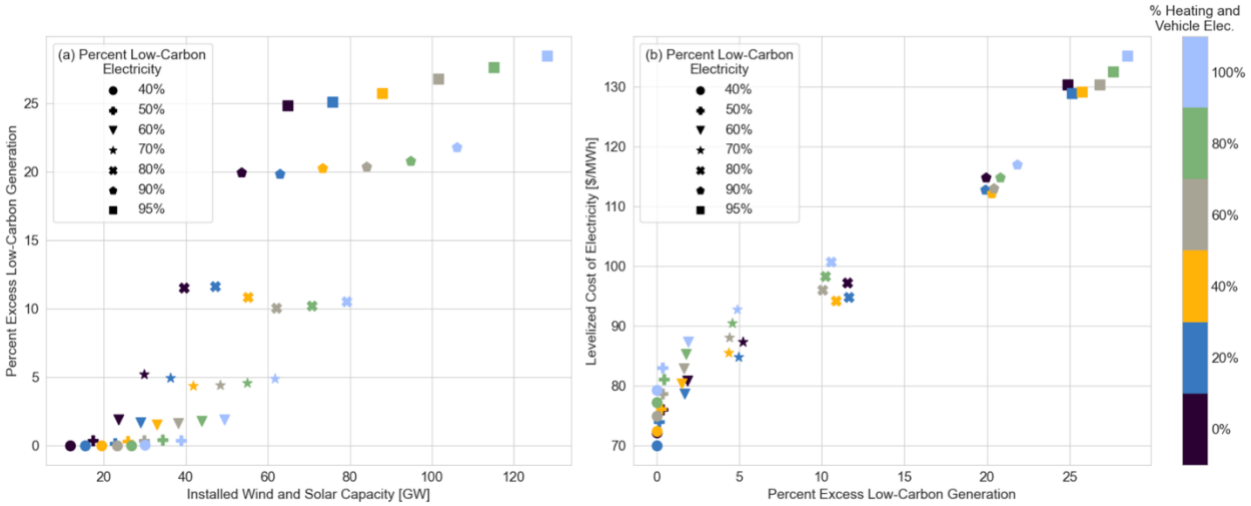

Fig. 4: (a) Average percent excess low-carbon generation for the entire 6-year simulation period *vs. installed wind and solar capacity; (b) LCOE vs. percent excess low-carbon generation. Results*

are shown for the same independent decarbonization scenarios in Fig. 3, whereby the low-carbon electricity percent and the rate of heating and vehicle electrification are set, and SECTR-NY determines the least-cost energy system.

The results presented thus far show how electrification accompanied by a significant buildout of renewable energy can keep LCOE low. On the other hand, a focus on large LCP fractions beyond 70% represents a major cost escalation. Competing drivers and trade-offs are next examined among scenarios with increasing HVE while maintaining LCP at 60% (Fig. 5(a-d)) vs. scenarios where HVE is 40% and LCP is progressively increased (Fig. 5(e-h)). (The trends observed here hold for other combinations of HVE and LCP; see Supplementary Figures S7-S8.) Fig. 5(a-d) demonstrates the stable buildout of generation capacity and consistency of system behavior and costs as electrification increases. In order to meet the increased demand, low-carbon generation, gas generation, and battery capacity all increase with electrification, per Fig. 5(a); gas generation undergoes the largest capacity increase – from 27.0 GW to 67.2 GW at 100% HVE – in order to meet higher electrification-induced demand peaks. Here, additional gas capacity is selected due to its low cost relative to the model's other dispatchable generation option, battery storage. With additional policy-based constraints in place, such as a limit on additional gas turbine capacity or demand-side strategies to mitigate peak heating loads, much less new gas capacity would be built out. Electricity generation trends (Fig. 5(b)) largely mirror the expansion in generation capacity, with the ratio of solar to wind generation (combined onshore and offshore) staying consistent from 0.31 at 0% HVE to 0.34 at 100% HVE, although with an increasing amount of wind generation coming from offshore capacity. Fig. 5(d) reveals the reason for consistency in system behavior: Despite increasing average uncurtailed low-carbon electricity generation from 9.5 GWh/h at 0% HVE to 17.7 GWh/h at 100% HVE, average excess low-carbon generation only increases from 177 MWh/h to 336 MWh/h. Electrification thus supports renewable energy integration by keeping the LCOEs of those supply resources low (Fig. 5(c)).

Conversely, optimal energy system characteristics change substantially with increasing LCPs. The previously noted inflection point at 70-80% LCPs is characterized by a large increase in battery capacity (Fig. 5(e)): Of the 33.4 GW of installed battery capacity at 95%, 26.1 GW is installed between 80% and 95%. As implied by Fig. 4, this buildout is due to the significant increase in excess low-carbon generation shown in Fig. 5(h). Furthermore, as battery capacity increases, battery energy throughput does not increase as much (Fig. 5(f)), resulting in battery LCOE growth from $117/MWh at 80% LCP to $198/MWh at 95% LCP (Fig. 5(g)). Similarly, gas-based generation capacity remains fairly steady even at very high LCPs, but the electricity generation from that capacity decreases significantly. The result is gas generation LCOE steadily increasing from $57/MWh at 40% LCP to $72/MWh at 70% LCP and accelerating to $260/MWh at 95% LCOE. It is worth noting that these results partially reflect the constraints of the model; they suggest that other technologies not included in SECTR-NY due to their non-competitive costs become beneficial in pushes to eliminate emissions from electricity generation. Regardless, these technology costs coupled with the significant increase in wind and solar LCOEs due to curtailment give a strong indication of the dominance of integration costs at high LCP.

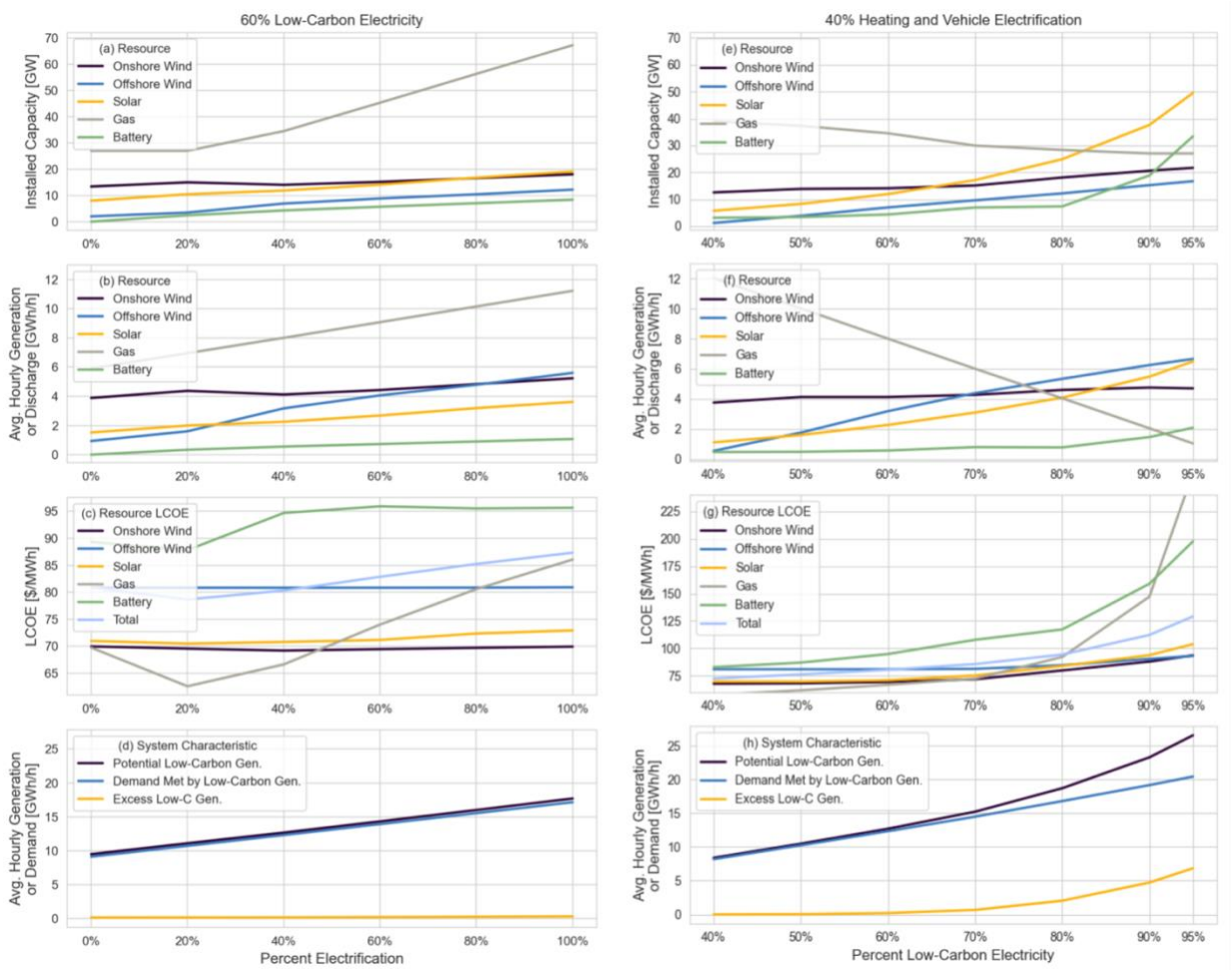

Fig. 5: System characteristics for scenarios with (a-d) increasing HVE at 60% LCP; and (e-h) increasing LCP at 40% HVE. Subplots (a, e) present installed capacity; (b, f) present average generation by resource; (c, g) present LCOE per MWh for the generation and storage resources; and (d, h) present demand and generation quantities. In (c, g), resource LCOE for onshore wind, offshore wind, and solar refers to the LCOE of generation; LCOE for battery storage is per-MWh discharge; total LCOE contains all system costs; and in (c), gas generation LCOE at 95% LCP ($260/MWh) is cropped out to preserve y-axis resolution.

Fig. 6 shows the monthly low-carbon electricity supply for (a) 60% LCP for HVEs of 0%, 40% and 80%, and (b) 40% HVE for LCPs of 60%, 80% and 95%. The seasonal low-carbon supply in Fig. 6(a) is nearly identical regardless of HVE and is largely in line with wind supply patterns shown in Fig. 2; this holds despite the low-carbon generation supply increasing 68% between HVEs of 0% and 80%. Accordingly, low-carbon electricity supply phenomena are shown to be essentially independent of HVE, despite very significant shifts in diurnal and seasonal demand patterns with HVE. In contrast, Fig. 6(b) shows a significant shift in seasonal low-carbon supply behavior reflecting the increased share of solar shown in Fig. 5(f). (Additional system operation characteristics were investigated on this monthly timescale to inform the findings here; given space considerations, these have been included in Supplementary Figures S3-S5.)

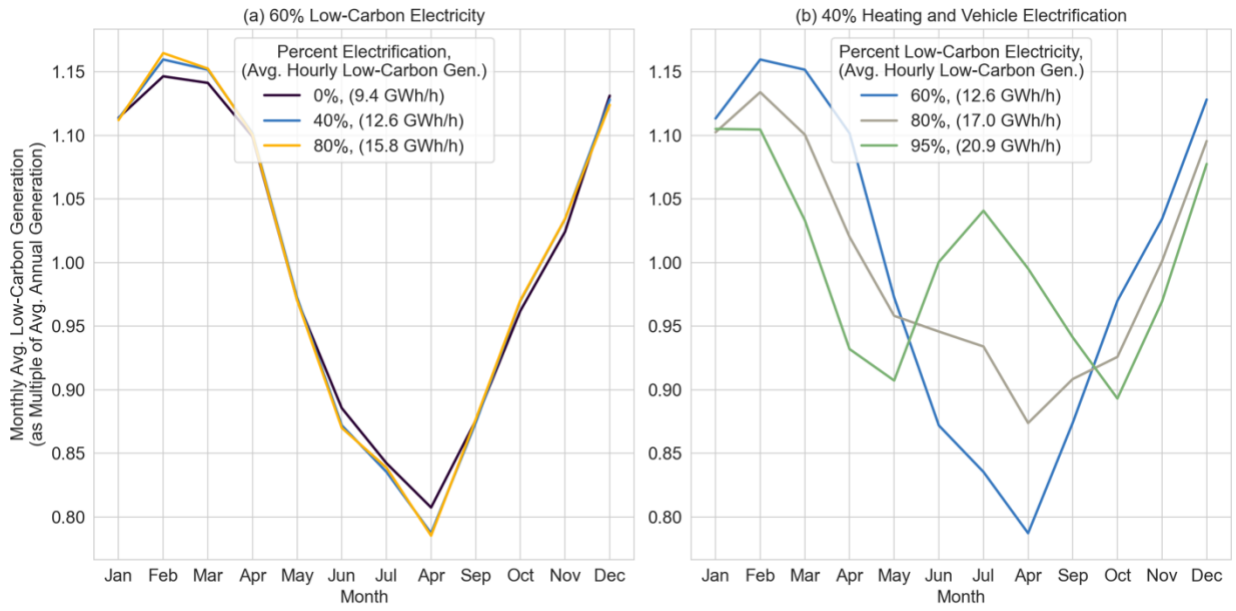

Fig. 6: Monthly average low-carbon generation as a multiple of the average annual low-carbon generation. (a) monthly averages for 0%, 40%, 80% HVEs at 60% LCP; (b) monthly averages for 60%, 80%, and 95% LCPs at 40% HVE.

Solar's contribution to the overall supply mix increases most dramatically beyond 80% LCP as battery storage increases: whereas 19.2 GW of solar capacity is installed between 40% and 80% LCP, 24.6 GW of capacity is installed just between 80% and 95% LCP (see Fig. 5(e)). This reflects complex dynamics in which overall system behavior may mask unique marginal behaviors of individual components: the operation of the same resource at lower LCP may be quite different with other resources present at higher LCPs. To this end, the paired buildout of solar and battery capacity at very high LCPs provides the most cost-effective method of displacing the remaining gas generation, as the daily cycling of solar generation allows for regular battery charging during the day and discharging at night even as it becomes the highest LCOE renewable resource (Fig. 5(g)). Fig. 7 shows how battery behavior and its relation to wind and solar supply changes at increasing LCPs for a given 40% HVE. (See Supplementary Figures S9-S10 for other HVEs, which show the same trends as Fig. 7.)

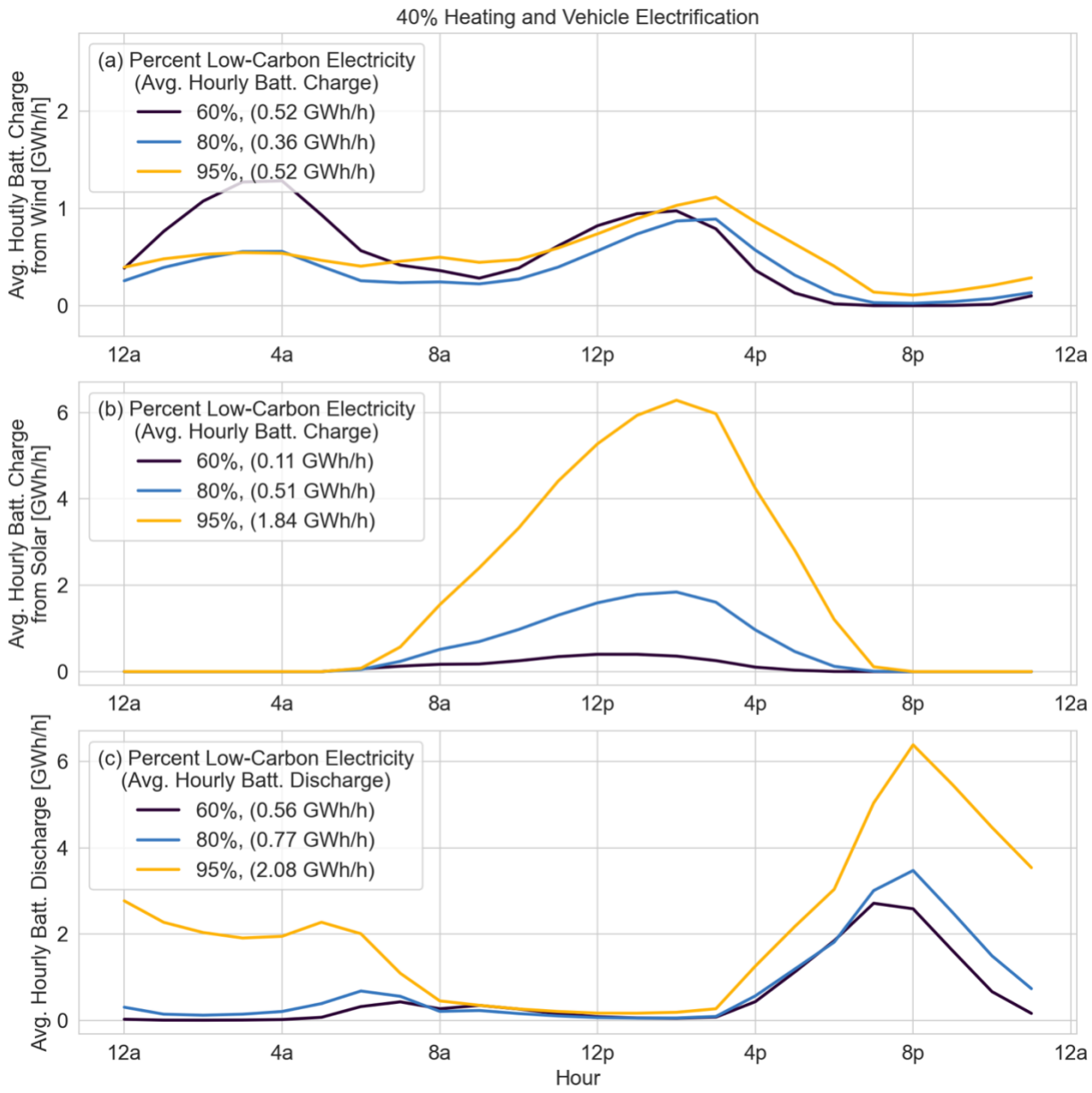

Fig. 7: Average battery operation by hour for 60%, 80%, and 95% LCPs over the entire 6-year simulation period*. (a) average hourly battery charging from wind (note y-axis scale is unique from (b) and (c)); (b) average hourly battery charging from solar; and (c) average battery discharge, all in GWh/h.*

At 60% LCP in Fig. 7, when total wind supply is roughly three times total solar supply, battery charging from wind is approximately 5 times higher than solar with distinct overnight and afternoon charging periods. At 80% LCP, wind's overnight charging reduces while both wind and solar charge the batteries in the afternoon; battery charging from solar becomes 1.4 times that from wind despite total wind supply being 2.4 times solar supply. Despite this shift between 60% and 80% LCP, the battery discharge remains almost entirely in the evening while total battery throughput increases by 38%. From 80% to 95% LCP, the maximum hourly average discharge in

the evening doubles from 3 GWh/h to 6 GWh/h, extending throughout the night with a steady average 2-3 GWh/h supply resulting in a near tripling of the total throughput. The additional energy supply to the battery comes almost entirely from solar: While total wind supply remains 1.8 times the solar supply, battery charging from solar is 3.5 times that from wind. Here, the diurnal pattern of solar generation allows for daily battery cycling and higher battery throughput, behavior that enables the integration of more low-carbon generation.

While the average diurnal behavior shown in Fig. 7 is useful in understanding broad system behavior and the results of model decisions, decision-making is often based on complex dynamics occurring at hourly timescales over particular periods of time that set capacity and operational needs. Figs. 8 and 9 show representative weeks in the winter and summer, respectively: The upper figures (Figs. 8(a) and 9(a)) show scenarios of 80% LCP and 40% HVE, and the lower figures (Figs. 8(b) and 9(b)) show scenarios of 95% LCP and 40% HVE. Fig. 8(a) shows that the lowest LCOE low-carbon option of wind provides much of the winter energy needs at 80% LCP, due to the resource's high seasonal productivity. Conversely, there are higher needs for gas-based generation in the summer (Fig. 9(a)). In both figures, curtailment (i.e., slack in the SECTR-NY energy balance constraint) is attributed to solar and wind in proportion to their hourly generation; however, as noted in the discussion around Fig. 7, the natural pairing of solar generation and battery storage means that more wind generation is curtailed relative to solar.

As the LCP increases to 95% (Figs. 8(b) and 9(b)), the reason for coupling more solar power with battery storage is revealed: Solar generation exceeding demand during the afternoon is used to charge battery storage, which is then discharged to meet evening demand (and overnight demand, if enough stored energy is available). In Figs. 8(b) and 9(b), approximately 5% of demand met by gas generation occurs during extended hours of low wind production. Here, batteries are not as cost-effective in displacing gas generation: low wind generation potentials lasting a day or longer would require multi-day battery cycling periods, and accordingly, underutilization of storage capacity relative to its usage with solar. (For further exploration that reinforces this interpretation, Supplementary Figures S11-S12 present the same representative week and LCPs as Figs. 8-9 but at 80% HVE.)

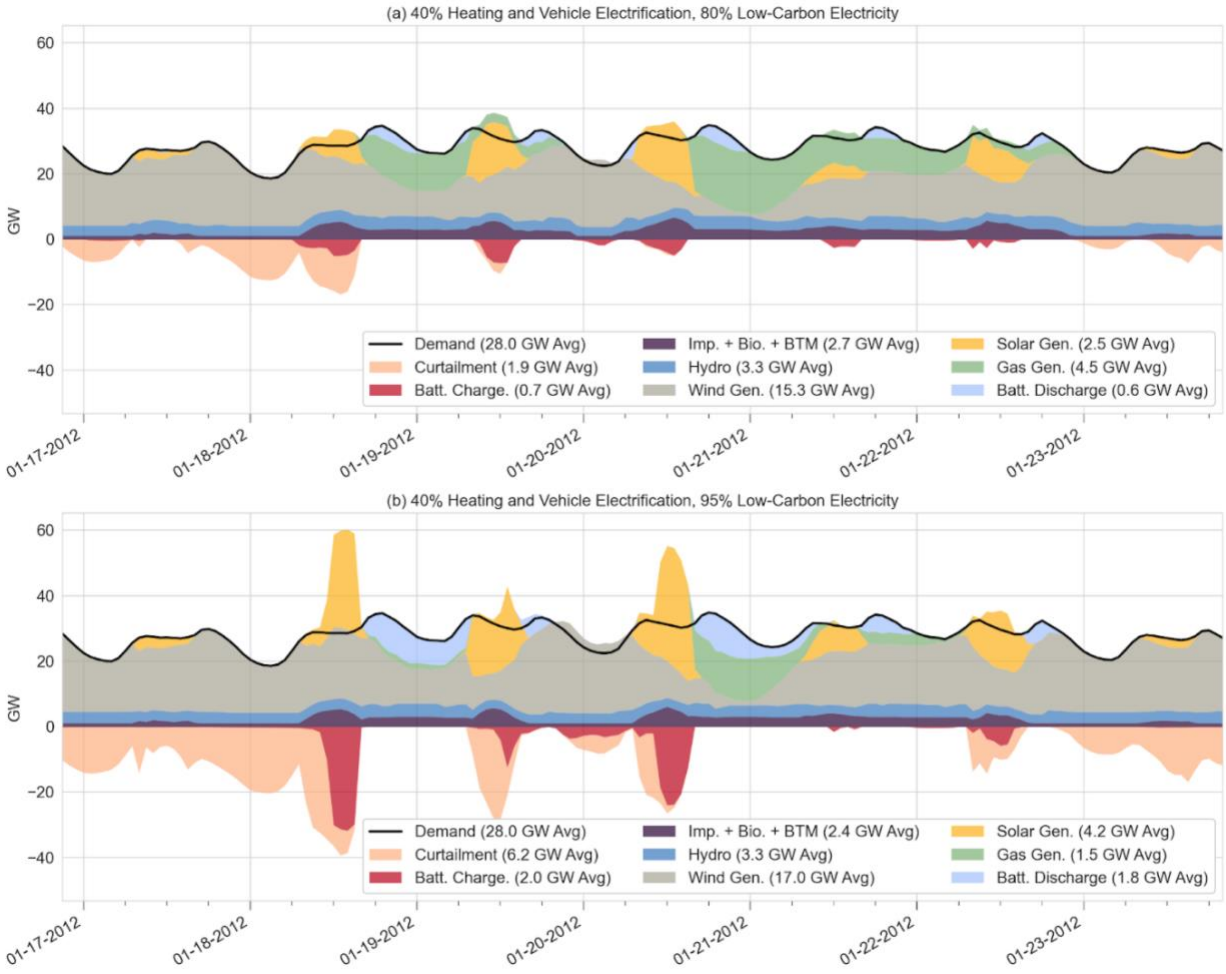

Fig. 8: Electricity generation and demand for a representative winter week with 40% HVE. (a) 80% LCP; (b) 95% LCP. 'Imp. + Bio. + BTM' represents the sum of imports, biofuel, and behind-the-meter solar generation. Average values reported in the legend are for the week shown.

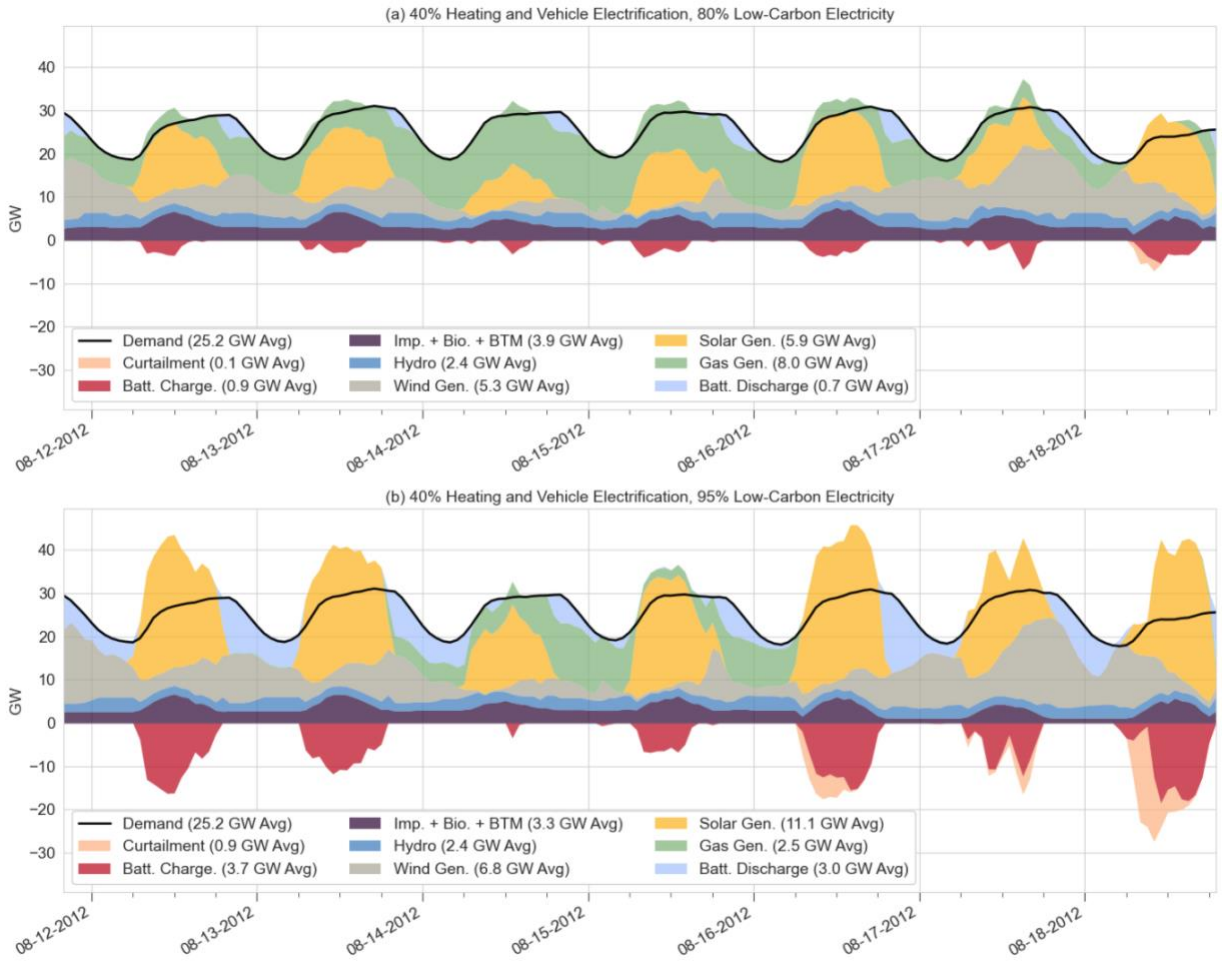

Fig. 9: Electricity generation and demand for a representative summer week with 40% HVE. (a) 80% LCP; (b) 95% LCP. 'Imp. + Bio. + BTM' represents the sum of imports, biofuel, and behind-the-meter solar generation. Average values reported in the legend are for the week shown.

3.3 Comparison to New York State policy studies

SECTR-NY model results are compared to initial analyses presented to the New York State Climate Action Council[v], a committee preparing a scoping plan for CLCPA, both to validate SECTR-NY outputs and to evaluate the effects of different model assumptions and input data. A comparison of select characteristics of the NYS Climate Action Council Advisory Panel (AP) 2030 scenario and two SECTR-NY scenarios is shown in Table 3. The AP 2030 scenario includes an 85% LCP and approximately 15% HVE[vi] with a computed energy-related GHG emissions reduction of 47.4% (relative to 1990, as are all GHG reductions discussed here); this scenario includes 28.4 GW of total wind and solar capacity and 3 GW battery storage capacity. For the same LCP and HVE, SECTR-NY Scenario A computes a total wind and solar capacity of 39.2 GW, 3.2 GW battery storage capacity, and GHG emissions reduction of 27.7%. There are two primary drivers for the greater SECTR-NY capacities here:

1. 14% higher average total wind and solar generation in SECTR-NY Scenario A (9.0 GW) than in AP 2030 (7.9 GW). This is due to more hydropower generation in AP 2030 than in the historical data used in SECTR-NY [39] and approximately 2.3 GW higher average statewide load in SECTR-NY Scenario A. The latter stems from a combination of SECTR-NY using historical electricity demand timeseries containing a higher existing average load (18.7 GW) than is simulated in NYS studies (18.2 GW); 15% SECTR-NY HVE likely being slightly higher than the estimate for AP 2030; AP 2030 considering combinations of population growth and efficiency savings; and SECTR-NY's more accurate representation of low-temperature effects of EHPs and EVs. (These low-temperature effects also explain the difference in fossil fuel-based generation capacity to meet the 35.4 GW peak statewide load computed in SECTR compared to the 29.6 GW statewide peak in AP 2030.)
2. 21% higher aggregate wind and solar capacity factor (CF) in AP 2030 (0.278) than in SECTR-NY Scenario A (0.230). This is primarily driven by significantly lower solar and onshore wind CFs in the latter. Model wind output in SECTR-NY is less than that of most available wind data: SECTR-NY employs a dataset that contains adjusted model data based on historical output of actual wind farms in NYS [40]. A comparison of solar data series was not performed; however, the authors believe SECTR-NY Scenario A's statewide solar CF of 0.166 represents more realistic expectations for NYS's latitude range than AP 2030's 0.194.

The difference in computed GHG reductions between AP 2030 and SECTR-NY Scenario A stems from model assumptions related to methane leakage in natural gas production and transport upstream of NYS. SECTR-NY relies on research on natural gas leakage [41,42] that estimates approximately 3.6% leakage with an associated impact on fossil fuel emissions factors [43]. AP 2030 reduces the leakage to approximately 2%, though the authors have not seen an explanation for this assumption. The implications of these assumptions can be seen in SECTR-NY Scenario B, in which more heating and vehicle electrification is needed to achieve the same percentage GHG

[v] NYS published studies are available at the following link: https://climate.ny.gov/Climate-Resources. Technical analysis of initial results [31] and of key drivers and outputs [46] last updated in November and December of 2021 are of particular use in understanding the state's modeling methodology and simulated decarbonization pathways.
[vi] The AP considered different electrification rates for different end uses, so this estimate is not directly analogous to that of SECTR-NY presented here. See Table 3, footnote 2 for a breakdown of the different electrification rates assumed in the AP recommendations.

emissions reduction as that computed for AP 2030. Here, total computed wind and solar capacity increases to 51.4 GW, 81% greater than that anticipated by the recent analyses presented to the NYS Climate Action Council.

Table 3: Comparison of NYS Climate Action Council Advisory Panel (AP) recommendations and SECTR-NY simulation results for modeled 2030 decarbonization scenarios.

	Modeled Scenario		
	NYS AP 2030	SECTR-NY, A	SECTR-NY, B
Low-Carbon Electricity Percent (LCP)	85%	85%[1]	85%[1]
Heating and Vehicle Electrification (HVE)	15%[2]	15%[1]	50%
GHG Emissions Change (Compared to 1990)	-47.4%	-27.7%	-47.4%[1]
Electricity Demand Peak [GW] | Average [GWh/h]	29.6 |18.4	35.4 | 20.7	52.7 | 25.4
Onshore Wind Capacity [GW] | Average Generation [GWh/h]	5.2 | 1.7	11.2 | 2.6	14.2 | 3.4
Offshore Wind Capacity [GW] | Average Generation [GWh/h]	6.2 | 2.9	8.4 | 3.8	13.2 | 5.8
Solar Capacity [GW] | Average Generation [GWh/h]	17.0 | 3.3	19.6 | 2.7	24.0 | 3.9
In-State Hydropower Capacity [GW] | Average Generation [GWh/h]	4.6 | 3.5	5.3 | 3.0	5.3 | 3.0
Hydropower Imports Capacity [GW] | Average Generation [GWh/h]	2.7 | 2.2	2.8 | 2.0	2.8 | 2.0
Nuclear Capacity [GW] | Average Generation [GWh/h]	3.4 | 3.0	3.5 | 3.2	3.5 | 3.2
Battery Capacity [GW]	3.0	3.2	9.9
Fossil Fuel Capacity [GW] | Average Generation [GWh/h]	20.8 | 2.7	27.0 | 2.5	27.6 | 3.2

[1] Indicates configuration parameters specified for the SECTR-NY model scenario.

[2]Approximated from the following proportions of vehicle and building stock end use equipment transitioning to electric alternatives in the AP 2030 scenario: 14% of light duty vehicles, 6% of heavy duty vehicles, 11% of residential space heating; 11% of commercial space heating, 25% of residential water heating, and 19% of commercial water heating.

4. Discussion

This study's results are broadly consistent with previously published research that deep greenhouse gas (GHG) emissions reductions require both a significant low-carbon electricity percentage (LCP) and increases in heating and vehicle electrification (HVE); however, an important finding is that by prioritizing heating and vehicle electrification in conjunction with renewable energy deployment rather than first focusing on LCP, emissions reductions can be achieved with lower electricity supply costs. Through comparative scenarios, the benefits of end use electrification to the electricity system are emphasized: Heating and vehicle electrification allows the same amount of renewable energy to be installed with significantly lower electricity supply costs all while producing deeper reductions in GHG emissions.

First order GHG reductions from electrification occur because of improved energy efficiency compared to the direct use of fossil fuels for heating and vehicles, even when the LCP is close to 40%, i.e. that of the existing NYS electricity grid. At this LCP, average heating emissions per unit heat delivered are 70% lower with current electric technologies than existing fossil fuel-based heating; average vehicle emissions per mile traveled are 56% lower.

For LCPs at or below 60%, higher levelized costs of electricity (LCOE) of wind and solar generation are mitigated by higher utilization of existing infrastructure with increased HVE (with LCOE even decreasing at HVEs up to 20-40%). The 70-80% LCP range represents a transition phase: Beyond 80%, integration costs (e.g., curtailment and battery storage) lead to rapidly rising LCOEs. Accordingly, three primary levelized cost of electricity (LCOE) drivers are identified from the range of LCPs and HVEs investigated: (1) per-unit costs of existing infrastructure decrease with increasing demand from HVE, (2) wind and solar power generation costs rise relative to gas-based and hydropower generation, and (3) costs of integration increase when large amounts of wind and solar power produce electricity in excess of demand.

For LCPs below 80%, wind generation meets most of the low-carbon generation requirement, as onshore wind represents the lowest LCOE renewable resource, followed by offshore wind resources near the dense load areas of New York City and Long Island. Beyond 80% LCP, paired solar generation and batteries become the most cost-effective method of displacing fossil fuel-based electricity generation. At higher LCPs, battery cycling occurs daily, making solar a more appropriate paired generation resource – at least some electricity is generated from solar daily whereas wind can drop off considerably for multi-day periods, particularly in the summer.

The marginal costs of lowering emissions from the limited set of electricity supply technologies considered here (wind, solar, battery and gas turbines) become high enough at LCPs larger than 80% to suggest that other nascent technologies (e.g., hydrogen storage) may play a role in achieving full energy sector decarbonization. Moreover, targeted deployment of other demand-side technologies not modeled – such as upgraded building envelopes, thermal storage and ground-source heat pumps – could further reduce supply costs by reducing heating-driven system peaks. Demand-side flexibility measures – like dual-fuel capabilities and grid-interactive

controls – may also mitigate integration costs and reduce dispatchable capacity requirements. Lastly, breakthroughs in energy and emissions intensive industrial sectors could partially scale down emissions reductions needed in the residential, commercial, transportation, and electricity sectors.

A comparison of model results described in this paper to initial analyses presented to the New York State Climate Action Council ("NYS study") validated SECTR-NY outputs, but also highlighted important factors in assessing the planning implications of such models. While SECTR-NY and the NYS study compute similar energy resource capacities for a scenario in line with the State's Year 2030 targets, deviations between the two can largely be attributed to differences in time series data for wind/solar potential time series and historical demand data, and to this paper's particular attention to low-temperature effects on heat pump and electric vehicle performance. Accurately modeling the potential generation from renewable resources and new electrification-driven peak demands does thus affect the resource capacity required to meet the electric load. However, the two models do diverge significantly in the calculation of GHG emissions. SECTR-NY computes lower emission reductions than the NYS study for a given combination of LCP and HVE; SECTR-NY includes upstream natural gas leakage in line with recent research and its related quantifiable GHG effects, whereas the NYS study assumes a lower leakage rate. As detailed in the paper, this distinction has significant implications for the amount of electrification needed to meet the State's GHG reduction targets.

A couple of caveats surrounding this paper's methodology and results are also worth mentioning. Foremost, SECTR does not model the electricity distribution network. As there will be a need to upgrade distribution to incorporate end-use heating and vehicle electrification, future work should investigate the scale, location, and costs of this reinforced capacity. Second, all SECTR generation is considered to be lumped. While this assumption substantially increases model tractability, it masks operating practices at the individual generator level where decisions are made. Third, LCPs are imposed on the amount of instate electricity generation, and do not account for the carbon content of any imported electricity. Should state regulations change to allow clean, imported electricity to satisfy low-carbon generation targets, the SECTR general formulation will need to be adjusted. Lastly, this paper presents results for a single set of cost assumptions. Should these assumptions prove inaccurate, rerunning the presented decarbonization scenarios will be required.

As the SECTR framework is an open-source, computationally efficient, capacity transition and system operation framework, the energy systems research community can adapt it in a number of ways for future work. One possibility is parameterizing SECTR for other RTO/ISO settings to explore comparative lowest cost decarbonization pathways. Moreover, within an RTO/ISO, researchers can investigate the impact of further interconnections to external generation. Lastly, researchers can build upon the SECTR framework by addressing the caveats mentioned above, such as by adding location specific costs for upgraded distribution capacity.

5. Conclusions

This paper introduces an open-source System Electrification and Capacity Transition (SECTR) modeling framework; the framework is then applied to the New York State (NYS) regional energy system (SECTR-NY). By characterizing existing system capacities, loads, and pricing structures, SECTR-NY reasonably approximates current electricity supply costs, establishing a reliable baseline from which to investigate different combinations of low-carbon electricity percentages (LCP) and heating and vehicle electrification rates (HVE).

Methodologically, SECTR addresses several shortcomings of traditional capacity expansion models (CEMs), including characterization of existing energy infrastructure systems, multi-year simulations with weather-dependent time series inputs, and spatially resolved end-use electrification effects. In parameterizing the model for NYS, the model incorporates improved emissions accounting assumptions specified by recent climate legislation but previously unimplemented in state decarbonization studies. This study demonstrates that overall energy emissions reductions can be achieved at lower electricity costs by prioritizing heating and vehicle electrification ahead of complete grid decarbonization; the former approach still requires a major buildout of wind and solar power, but at lower percentage penetration into the grid because of higher demands from more electrification. Moreover, three main electricity supply cost drivers are established for a decarbonizing energy system: (1) decreasing per-unit supply costs of existing infrastructure with increasing electrification (i.e. with higher demand); (2) higher wind and solar power supply costs relative to current hydropower and fossil fuel-based generation; and (3) increasing costs of integration (due to curtailment and energy storage) as solar and wind supply in excess of demand increase with LCP.

6. Data Availability

All code and data used for the SECTR-NY model formulation can be found in the following GitHub repository: https://github.com/SEL-Columbia/sectr-ny.

7. Acknowledgements

Partial support for this effort was provided by the National Science Foundation. T.C. received support through INFEWS NSF Award Number 1639214; M.B.W. received support through SRN NSF Award Number 1444745.

V.M. and M.B.W received support through Breakthrough Energy Grant Number BE CU20-3670.

7. Appendix A

Table 4 contains a full listing of all nodal cost assumptions in SECTR-NY. The Supplementary Materials provides a full accounting of how these assumptions were reached. Internodal transmission upgrade and O&M costs are presented in Supplementary Table S2.

Table 4: Cost assumptions used in SECTR-NY.

Quantity	Unit	Node 1 ($)	Node 2 ($)	Node 3 ($)	Node 4 ($)	Notes
Onshore Wind Capacity Cost, High	$/kW	1992	1992	N/A	N/A	See SM, page 18
Onshore Wind Capacity Cost, Low	$/kW	1698	1698	N/A	N/A	See SM, page 18
Offshore Wind Capacity Cost, High	$/kW	N/A	N/A	3583	3583	See SM, page 18
Offshore Wind Capacity Cost, Low	$/kW	N/A	N/A	2256	2256	See SM, page 18
Utility-Scale Solar Capacity Cost, High	$/kW	1341	1341	1593	1593	See SM, page 19
Utility-Scale Solar Capacity Cost, Low	$/kW	1006	1006	1195	1195	See SM, page 19
Battery Storage Energy Cost, High	$/kWh	208	208	208	208	See SM, page 21
Battery Storage Energy Cost, High	$/kWh	144	144	144	144	See SM, page 21
Hydrogen Storage Energy Cost	$/kWh	0.35	8.29	8.29	8.29	See SM, page 22
Hydrogen Storage Power Cost	$/kW	3013	3013	4036	4036	See SM, page 22
New Fossil Fuel-Based Generation Capacity Cost	$/kW	772	772	1034	1034	See SM, page 17
Hydropower Generation Cost	$/MWh	18.47	28.02	N/A	N/A	See SM, page 23
Nuclear Generation Cost	$/MWh	37.94	N/A	26.82	N/A	See SM, page 22
Biofuel Generation Cost	$/MWh	20.66	27.41	27.05	32.39	See SM, page 24
Imported Electricity Cost	$/MWh	22.13	N/A	70	N/A	See SM, page 25
Wholesale Natural Gas Price	$/MMBTU	2.89	4.04	3.67	3.62	See SM, page 17
Existing Fossil Fuel-Based Generation Ramping Cost	$/MW-h	79	79	79	79	See SM, page 17
New Fossil Fuel-Based Generation Ramping Cost	$/MW-h	69	69	69	69	See SM, page 17
New Fossil Fuel-Based Generation Fixed O&M Cost	$/kW-yr	6.97	6.97	6.97	6.97	See SM, page 17
Onshore Wind Capacity Fixed O&M Cost	$/kW-yr	18.1	18.1	N/A	N/A	See SM, page 18
Offshore Wind Capacity Fixed O&M Cost	$/kW-yr	N/A	N/A	38	38	See SM, page 18
Utility-Scale Solar Capacity Fixed O&M Cost	$/kW-yr	10.4	10.4	10.4	10.4	See SM, page 19
Hydrogen Storage Fixed O&M Cost	$/kW-yr	48.87	48.87	48.87	48.87	See SM, page 22
New Fossil Fuel Based Generation Variable O&M Cost	$/MWh	4.48	4.48	4.48	4.48	See SM, page 17
Existing Generation Capacity Maintenance Cost	$/kW-yr	27.64	53.44	101.303	104.6	See SM, page 17
Existing Transmission Capacity Maintenance Cost	$/MWh	16.9	16.9	27.3	27.3	See SM, page 17

Table 5 contains a full listing of existing nodal capacities modeled in SECTR-NY. The Supplementary Materials provides a full accounting of how these values were reached. Internodal existing transmission capacities are presented in Supplementary Table S2.

Table 5: Existing capacities modeled in SECTR-NY.

Capacity Type	Node 1 (MW)	Node 2 (MW)	Node 3 (MW)	Node 4 (MW)	Notes
Onshore Wind	1985	0	0	0	See SM, page 18
Offshore Wind	0	0	0	0	See SM, page 18
Utility Scale Solar	0	0	0	56.5	See SM, page 19
Behind-the-Meter Solar	562	523	293	259	See SM, page 20
Gas-Fueled	3934.2	8622.5	10249.9	4192.7	See SM, page 17
Hydropower	4717.4	608.7	0	0	See SM, page 23
Nuclear	3536.8	0	2311	0	See SM, page 22
Biofuel	258	45	59.7	142.2	See SM, page 24
Interregional Import Limits	1500	0	1250	0	See SM, page 25
Battery Storage, Energy	5.2	80	0	65	See SM, page 21
Battery Storage, Power	3	20	0	10	See SM, page 21

7. References

[1] Clack CTM, Choukulkar A, Cote B, McKee SA. Technical Report: Economic & Clean Energy Benefits of Establishing a Competitive Wholesale Electricity Market in the Southeast United States 2020:153. https://vibrantcleanenergy.com/wp-content/uploads/2020/08/SERTO_WISdomP_VCE-EI.pdf.

[2] Clean Air Task Force. State and utility climate change targets shift to carbon reductions 2019:1–9. https://www.catf.us/wp-content/uploads/2019/05/State-and-Utility-Climate-Change-Targets.pdf.

[3] Scovronick N, Budolfson M, Dennig F, Errickson F, Fleurbaey M, Peng W, et al. The impact of human health co-benefits on evaluations of global climate policy. Nat Commun 2019;10:1–12. https://doi.org/10.1038/s41467-019-09499-x.

[4] Fitzroy F. A Green New Deal: The Economic Benefits of Energy Transition. Substantia 2019;3(2) Suppl:55–67. https://doi.org/10.13128/Substantia-276.

[5] Tyson A, Kennedy B. Two-Thirds of Americans Think Government Should Do More on Climate. Pew Res Cent 2020. https://www.pewresearch.org/science/2020/06/23/two-thirds-of-americans-think-government-should-do-more-on-climate/.

[6] Guelpa E, Bischi A, Verda V, Chertkov M, Lund H. Towards future infrastructures for sustainable multi-energy systems: A review. Energy 2019;184:2–21. https://doi.org/10.1016/j.energy.2019.05.057.

[7] Grubler A, Wilson C, Bento N, Boza-Kiss B, Krey V, McCollum DL, et al. A low energy demand scenario for meeting the 1.5 °C target and sustainable development goals without negative emission technologies. Nat Energy 2018;3:515–27. https://doi.org/10.1038/s41560-018-0172-6.

[8] Bistline JET. Roadmaps to net-zero emissions systems: Emerging insights and modeling challenges. Joule 2021;5:2551–63. https://doi.org/10.1016/j.joule.2021.09.012.

[9] Conlon T, Waite M, Modi V. Assessing new transmission and energy storage in achieving increasing renewable generation targets in a regional grid. Appl Energy 2019;250:1085–98. https://doi.org/10.1016/j.apenergy.2019.05.066.

[10] Barth R, Brand H, Meibom P, Weber C. A stochastic unit-commitment model for the evaluation of the impacts of integration of large amounts of intermittent wind power. 2006 9th Int Conf Probabilistic Methods Appl to Power Syst PMAPS 2006. https://doi.org/10.1109/PMAPS.2006.360195.

[11] Kern JD, Patino-Echeverri D, Characklis GW. An integrated reservoir-power system model for evaluating the impacts of wind integration on hydropower resources. Renew Energy 2014. https://doi.org/10.1016/j.renene.2014.06.014.

[12] An Y, Zeng B. Exploring the modeling capacity of two-stage robust optimization: Variants of robust unit commitment model. IEEE Trans Power Syst 2015;30:109–22. https://doi.org/10.1109/TPWRS.2014.2320880.

[13] Jenkins J, Sepulveda N. Enhanced Decision Support for a Changing Electricity Landscape: the GenX Configurable Electricity Resource Capacity Expansion Model. MIT Energy Initiat Work Pap 2017:1–40. https://energy.mit.edu/wp-content/uploads/2017/10/Enhanced-Decision-Support-for-a-Changing-Electricity-Landscape.pdf.

[14] Levi PJ, Kurland SD, Carbajales-Dale M, Weyant JP, Brandt AR, Benson SM. Macro-Energy Systems: Toward a New Discipline. Joule 2019;3:2282–6. https://doi.org/10.1016/j.joule.2019.07.017.
[15] Denholm P, Arent DJ, Baldwin SF, Bilello DE, Brinkman GL, Cochran JM, et al. The challenges of achieving a 100% renewable electricity system in the United States. Joule 2021;5:1331–52. https://doi.org/10.1016/j.joule.2021.03.028.
[16] Howells M, Rogner H, Strachan N, Heaps C, Huntington H, Kypreos S, et al. OSeMOSYS: The Open Source Energy Modeling System. An introduction to its ethos, structure and development. Energy Policy 2011;39:5850–70. https://doi.org/10.1016/j.enpol.2011.06.033.
[17] Gil E, Aravena I, Cardenas R. Generation Capacity Expansion Planning Under Hydro Uncertainty Using Stochastic Mixed Integer Programming and Scenario Reduction. IEEE Trans Power Syst 2015;30:1838–47. https://doi.org/10.1109/PESGM.2015.7285838.
[18] Short W, Sullivan P, Mai T, Mowers M, Uriarte C, Blair N, et al. Regional Energy Deployment System (ReEDS) - Technical Report. NREL 2011. https://www.nrel.gov/docs/fy12osti/46534.pdf.
[19] Karlsson K, Meibom P. Optimal investment paths for future renewable based energy systems-Using the optimisation model Balmorel. Int J Hydrogen Energy 2008;33:1777–87. https://doi.org/10.1016/j.ijhydene.2008.01.031.
[20] DeCarolis JF, Jaramillo P, Johnson JX, McCollum DL, Trutnevyte E, Daniels DC, et al. Leveraging Open-Source Tools for Collaborative Macro-energy System Modeling Efforts. Joule 2020;4:2523–6. https://doi.org/10.1016/j.joule.2020.11.002.
[21] Jenkins JD, Mayfield EN, Larson ED, Pacala SW, Greig C. Mission net-zero America: The nation-building path to a prosperous, net-zero emissions economy. Joule 2021;5:2755–61. https://doi.org/10.1016/j.joule.2021.10.016.
[22] Murphy C, Mai T, Sun Y, Jadun P, Muratori M, Nelson B, et al. Electrification Futures Study: Scenarios of Power System Evolution and Infrastructure Development for the United States. Natl Renew Energy Lab NREL/TP-6A20-72330 2021;1.
[23] Murphy C, Mai T, Sun Y, Jadun P, Donohoo-Vallett P, Muratori M, et al. High electrification futures: Impacts to the U.S. bulk power system. Electr J 2020;33:106878. https://doi.org/10.1016/j.tej.2020.106878.
[24] Steinberg D, Dave Bielen, Eichman J, Eurek K, Logan J, Mai T, et al. Electrification and Decarbonization: Exploring U.S. Energy Use and Greenhouse Gas Emissions in Scenarios with Widespread Electrification and Power Sector Decarbonization. Natl Renew Energy Lab 2017:43. https://doi.org/doi:10.2172/1372620.
[25] Zhou E, Mai T. Electrification Futures Study: Operational Analysis of U.S. Power Systems with Increased Electrification and Demand-Side Flexibility n.d. https://doi.org/10.2172/1785329.
[26] Mai T, Steinberg D, Logan J, Bielen D, Eurek K, McMillan C. An electrified future: Initial scenarios and future research for U.S. Energy and electricity systems. IEEE Power Energy Mag 2018;16:34–47. https://doi.org/10.1109/MPE.2018.2820445.
[27] Bellocchi S, Manno M, Noussan M, Prina MG, Vellini M. Electrification of transport and residential heating sectors in support of renewable penetration: Scenarios for the Italian energy system. Energy 2020;196:117062. https://doi.org/10.1016/j.energy.2020.117062.

[28] Eichman JD, Mueller F, Tarroja B, Schell LS, Samuelsen S. Exploration of the integration of renewable resources into California's electric system using the Holistic Grid Resource Integration and Deployment (HiGRID) tool. Energy 2013;50:353–63. https://doi.org/10.1016/j.energy.2012.11.024.
[29] Tarroja B, Chiang F, AghaKouchak A, Samuelsen S, Raghavan S V., Wei M, et al. Translating climate change and heating system electrification impacts on building energy use to future greenhouse gas emissions and electric grid capacity requirements in California. Appl Energy 2018;225:522–34. https://doi.org/10.1016/j.apenergy.2018.05.003.
[30] Environmental Economics and Energy. Pathways to Deep Decarbonization in New York State 2020. https://climate.ny.gov/-/media/Project/Climate/Files/2020-06-24-NYS-Decarbonization-Pathways-CAC-Presentation.ashx.
[31] New York State Climate Action Council. Technical Advisory Group, Integration Analysis -- Initial Results Presentation (updated November 21, 2021) 2021. https://climate.ny.gov/-/media/Project/Climate/Files/2021-11-18-Integration-Analysis-Initial-Results-Presentation.ashx.
[32] Giarola S, Molar-Cruz A, Vaillancourt K, Bahn O, Sarmiento L, Hawkes A, et al. The role of energy storage in the uptake of renewable energy: A model comparison approach. Energy Policy 2021;151:112159. https://doi.org/10.1016/j.enpol.2021.112159.
[33] Waite M, Modi V. Electricity Load Implications of Space Heating Decarbonization Pathways. Joule 2020;4:376–94. https://doi.org/10.1016/j.joule.2019.11.011.
[34] New York State Senate. Climate Leadership and Community Protection Act — Final Bill Text 2019. https://www.nysenate.gov/legislation/bills/2019/s6599.
[35] US Energy Information Administration (EIA). Annual Energy Outlook 2020 with projections to 2050. 2020. https://www.eia.gov/outlooks/aeo/pdf/aeo2020.pdf.
[36] Patton DB, LeeVanSchaick P, Chen J, Naga RP. 2019 State of the Market Report for the New York ISO Markets. Potomac Ecnonomics 2019:1–24. https://www.nyiso.com/documents/20142/2223763/NYISO-2019-SOM-Report-Full-Report-5-19-2020-final.pdf/.
[37] US Energy Information Administration (EIA). Electricity Data Browser 2021. https://www.eia.gov/electricity/data/browser/.
[38] Waite M, Modi V. Existing and projected infrastructure capacities motivate alternatives to all-electric heating decarbonization. Joule-D-19-00676 2019.
[39] US Energy Information Administration (EIA). Form EIA-923 detailed data with previous form data (EIA-906/920) 2020. https://www.eia.gov/electricity/data/eia923/.
[40] Waite M, Modi V. Modeling wind power curtailment with increased capacity in a regional electricity grid supplying a dense urban demand. Appl Energy 2016. https://doi.org/10.1016/j.apenergy.2016.08.078.
[41] Alvarez RA, Zavala-Araiza D, Lyon DR, Allen DT, Barkley ZR, Brandt AR, et al. Assessment of methane emissions from the U.S. oil and gas supply chain. Science (80-) 2018;361:186–8. https://doi.org/10.1126/science.aar7204.
[42] Howarth RW, Santoro R, Ingraffea A. Methane and the greenhouse-gas footprint of natural gas from shale formations. Clim Change 2011;106:679–90. https://doi.org/10.1007/s10584-011-0061-5.

[43] Howarth RW. Methane Emissions and Greenhouse Gas Accounting: A Case Study of a New Approach Pioneered by the State of New York 2019:14. https://documents.dps.ny.gov/public/Common/ViewDoc.aspx?DocRefId=%7B3498AB82-B671-451E-A556-A917A61F939A%7D.
[44] US Energy Information Administration (EIA). Annual household site end-use consumption by fuel in the U.S. 2018:8. https://www.eia.gov/consumption/residential/data/2015/c&e/pdf/ce4.1.pdf.
[45] US Energy Information Administration (EIA). Commercial Building Energy Consumption Survey (CBECS) 2018. https://www.eia.gov/consumption/commercial/data/2018/.
[46] New York State Climate Action Council. Technical Advisory Group, Integration Analysis -- Key Drivers and Outputs (updated December 30, 2021) 2021. https://climate.ny.gov/-/media/Project/Climate/Files/IA-Tech-Supplement-Annex-2-Key-Drivers-Outputs.ashx.